Retroviral transduction of HSCs and progenitors

The constructs of FLT3-ITD N51and FLT3-ITD tyrosine to phenylalanine mutant at sites 589 and 591, which are occult STAT5 binding sites, were previously described.[30] The retrovirus vector was transfected into 293T cells with gag and pol expression plasmids by $CaPO_4$ coprecipitation. The supernatant from transfected cells was collected after 48 hours and immediately stored at −80°C until use. FACS-purified murine HSCs were prestimulated in RPMI-1640 medium containing 20% FCS in the presence of murine (m) SCF (20 ng/mL), murine leukemia inhibitory factor (10 ng/mL) and mFL (10 ng/mL) for 18 hours. Cells were subsequently plated onto recombinant fibronectin fragment-coated culture dishes (RetroNectin dish; Takara) with 1 mL of virus supernatant containing identical cytokine cocktail and cultured for 48 hours. For progenitor transduction, FACS-purified cells were cultured for 48 hours on RetroNectin dishes with 1 mL of virus supernatant containing mSCF and mIL-11 (10 ng/mL) for GMPs

The enforced expression and knockdown experiments for MCL-1

Human MCL-1 cDNA plasmid was purchased from Open Biosystems. The coding sequence of MCL-1 in this plasmid was amplified by PCR using primers containing additional EcoRI site (5′-cggaattcggcaatgtttggcctc-3′) and BamHI site (5′-gcggatcctcttattagatatgc-3′) and cloned into pEGFP-C3 vector (Clontech). To suppress the expression level of MCL-1, we generated a vector that possesses expression cassettes of short hairpin (sh) RNA against MCL-1 using the BLOCK-iT PolII miR RNAi Expression Kit (Invitrogen) according to the manufacturer's recommendation. Target sequences were selected using BLOCK-iT RNAi Designer (Invitrogen). Briefly, oligonucleotides were synthesized to form shRNA on transcription, in order of sense, loop (lower case), and antisense sequences as follows: MCL-1 top strand oligo, 5′-tgctgttgatgtccagtttc-cgaagcgttttggccactgactgacgcttcggactggacatcaa-3′; MCL-1 bottom strand oligo, 5′-cctgttgatgtccagtccgaagcgtcagtcagtggccaaaacgcttcggaaactggacatcaac-3′. These oligonucleotides were annealed with their complementary ones and cloned subsequently into pcDNA 6.2-GW/EmGFP-miR expression vector. After confirming their sequences, expression vectors were transduced into MV4-11 cell lines by Amaxa Nucleofector System (Lonza). Cells (2×10^6) were suspended in 100 μL of Nucleofector solution with 2 μg of negative control vector or subcloned plasmid. Pulses were delivered with Nucleofector device using program Q-001 (Lonza).

STAT5 knockdown experiment

Double-stranded STAT5 siRNA was purchased from Invitrogen. STAT5 siRNA was transduced into MV4-11 cell lines by Amaxa Nucleofector System (Lonza). Cells (2×10^6) were suspended in 100 μL of Nucleofector solution with 1.5 μg of siRNA. Pulses were delivered with Nucleofector device using program Q-001.

Statistical analysis

Levels of significance were measured using paired *t* test.

Results

The phenotype of AML LSCs is preserved irrespective of FLT3-ITD expression

Among 30 AML samples enrolled in the study, FLT3-ITD was detected in 11 of 30 AML patients. The phenotypic characteristics are consistent in all AML cases analyzed irrespective of the presence of FLT3-ITD. Figure 1 shows the phenotypic analysis of normal and AML bone marrow cells. Patients' characteristics and their FACS data are summarized in Table 1. In normal BM, the HSC resides in the $CD34^+CD38^-Lin^-$ fraction that expresses Thy-1 (CD90) and c-KIT (CD117).[36-38] These $CD34^+CD38^-$ human HSCs uniformly express FLT3 (CD135), $CD45RA^-$, and IL-3Rα^{lo} $(CD123)^{lo}$ (Figure 1). Previous xenogeneic transplantation experiments showed that leukemia-initiating cells (leukemic

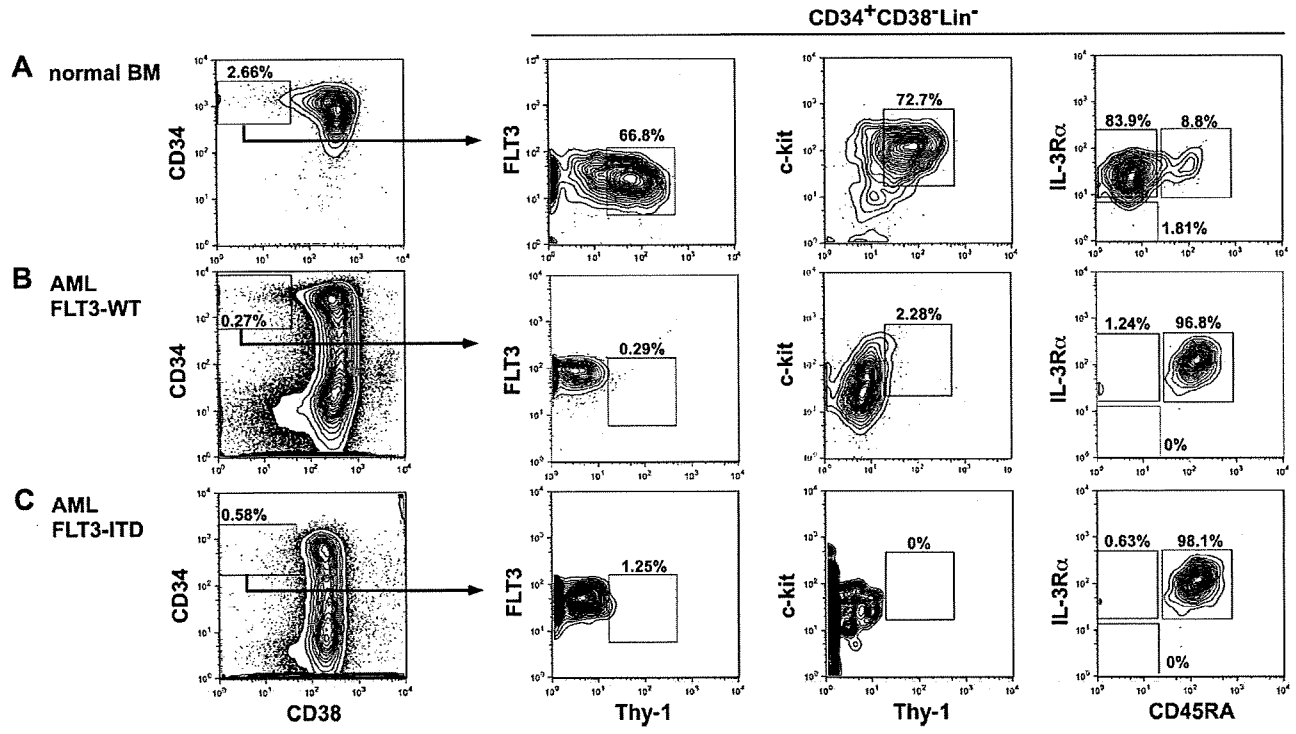

Figure 1. Stem and progenitor analysis of normal and AML bone marrow cells. Representative phenotype of the bone marrow cells in a normal control (A), FLT3-WT AML (B), and FLT3-ITD AML (C). Human $CD34^+CD38^-$ cells are enriched for normal HSCs with long-term reconstitution activity, and are Thy-1$^+$FLT3^{lo}c-KIT$^+$IL-3R$^+$$CD45RA^-$. In contrast, $CD34^+CD38^-$ AML LSCs were Thy-1$^-$ and expressed a high level of FLT3 compared with normal HSCs. The LSCs expressed a variety of levels of c-KIT, and were IL-3R$^+$$CD45RA^+$, resembling GMPs' phenotype. No significant difference in expression level of these molecules was found between FLT3-ITD and FLT3-WT AML LSCs.

Table 1. Patient characteristics

Patient no.	Age, y	Sex	FAB	Karyotype	WBC, $\times 10^9$/L	PB blast, %	BM blast, %	FLT3/ITD
1	38	M	M1	46, XY	67.0	92.5	85.6	−
2	35	M	M1	46, XY	4.9	22	76	−
3	34	M	M2	46, XY	3.7	9	38.4	−
4	27	M	M2	46, XY	25.8	82.7	67.3	−
5	57	M	M2	46, XY, del(20)(q11;q13)	2.2	1	21.6	−
6	57	M	M2	46, XY, +8	2.0	0	49.8	−
7	84	M	M2	45, XY, −7	3.8	41	64.8	−
8	32	M	M2	45, X, −Y, t(8;21)(q22;q22)	29.4	73.8	56.8	−
9	19	M	M2	46, XY, t(8;21)(q22;q22)	2.3	11	21.3	−
10	30	F	M2	45, X, −X, t(8;21)(q22;q22)	16.5	65	79.9	−
11	46	M	M2	46, XY, t(8;21)(q22;q22)	14.3	56	82.2	−
12	62	F	M3	46, XX, t(15;17)(q22;q21), add(18)(p11.2), add(20)(q13)	52.5	97	96	−
13	33	F	M3	46, XX, t(15;17)(q22;q21)	65.1	78	87.5	−
14	24	F	M3	46, XX, t(15;17)(q22;q21)	2.3	24	65	−
15	50	F	M4	46, XX	43.7	17	31.6	−
16	75	M	M4	46, XY	18.3	3	70	−
17	58	F	M5	46, XX, t(3;3)(q21;q26)	11.3	53	60	−
18	48	F	M5	49, XX, +8, t(9;11)(p22;q23), +14	1.6	23	90	−
19	71	M	M6	NA	4.5	1	28	−
20	86	M	M0	46, XY	17.3	63	92	+
21	84	F	M1	48, XX, +8	8.5	94	98	+
22	33	F	M1	46, XX	135.7	98	99.2	+
23	52	F	M1	46, XX	171.6	97	90	+
24	19	F	M2	46, XY, t(8;21)(q22;q22)	12.3	45	86	+
25	59	M	M3	46, XY, t(15;17)(q22;q21)	3.8	51	77.2	+
26	56	M	M3	46, XY, t(15;17)(q22;q21)	4.4	83	92.5	+
27	48	F	M4	46, XX	31.5	77.5	36	+
28	29	M	M4	46, XY	155.0	68.8	73	+
29	19	M	M4	46, XY	144.0	83.5	35	+
30	20	M	M7	46, XY	48.3	92	99	+

PB indicates peripheral blood; BM, bone marrow; M, male; and F, female.

stem cells [LSCs]) reside predominantly within the $CD34^+CD38^-Lin^-$ fraction of the AML bone marrow.[39,40] Interestingly, the entire $CD34^+CD38^-$ AML LSC fraction expressed FLT3 at a high level, whereas the majority of $CD34^+CD38^-$ LSCs expressed diversified levels of c-KIT in all 30 AML cases studied. $CD34^+CD38^-$ LSCs were negative for CD90 as reported.[41,42] They expressed a high level of CD45RA and CD123, resembling the phenotype of human GMPs[32] (Figure 1). Because anti-FLT3 antibodies react with the extracellular portion of FLT3-ITD as well as FLT3-WT, it is of note that FLT3-ITD protein is expressed in the $CD34^+CD38^-$ AML LSC fraction, indicating that FLT3-ITD signaling should operate at the LSC stage.

The presence of FLT3-ITD marks a fraction of AML with highest levels of MCL-1 expression

Figure 2 shows the real-time PCR analysis of MCL-1 mRNA levels in normal and leukemic BM mononuclear cells. AML BM cells expressed MCL-1 in all 30 cases at a level approximately 5-fold higher than that of normal BM cells, irrespective of their FAB types (Figure 2A). We have shown that, in normal human hematopoiesis, FLT3 signaling up-regulates MCL-1 but not BCL-2 and BCL-xL in HSCs and myeloid progenitors, promoting their cell survival.[10] Therefore, we hypothesized that the constitutive expression of FLT3 signaling by FLT3-ITD mutation can induce up-regulation of MCL-1 in the AML LSC fraction. As shown in Figure 2B, the level of MCL-1 mRNA in FLT3-ITD AML BM cells was higher than that of FLT3-WT AML by approximately 2-fold, suggesting that the presence of FLT3-ITD can mark a fraction of AML with a high level of MCL-1. The high-level expression of MCL-1 protein in FLT3-ITD AML blasts was confirmed by Western blot analysis (Figure 2C-D). FLT3-ITD AML cells expressed approximately 7- and approximately 3-fold higher levels of MCL-1 protein compared with normal BM and FLT3-WT AML cells, respectively. In human hematopoiesis, HSCs express the highest level of MCL-1, and its expression gradually declines as they differentiate into mature myeloid or lymphoid cells.[10] We therefore further subfractionated leukemic BM cells into $CD34^+CD38^-$ LSCs and $CD34^+CD38^+$ leukemic progenitor cell fractions. We could obtain sufficient numbers of cells for such analysis in 16 samples (10 cases of FLT3-WT and 6 cases of FLT3-ITD AMLs). As shown in Figure 3A, the $CD34^+CD38^-$ LSC fraction in FLT3-WT AMLs expressed approximately 6-fold higher, whereas those in FLT3-ITD AMLs had approximately 14-fold higher level of MCL-1, even compared with normal HSCs. In contrast, levels of BCL-2 and BCL-xL in the $CD34^+CD38^-$ LSCs and normal HSCs were not significantly different (Figure 3A). Cytoplasmic staining of MCL-1 FLT3-ITD AML LSC fraction shows that this population uniformly expressed MCL-1 protein at a high level on FACS, indicating that all single cells possessed high levels of MCL-1 (Figure 3B). Collectively, the $CD34^+CD38^-$ LSC fraction expressed the highest levels of MCL-1 in the leukemic BM.

FLT3 signaling stimulates MCL-1 expression in AML LSCs

Both FLT3 and c-KIT belong to the class III receptor tyrosine kinase family and share their major signaling cascade. Signals from either receptor play a critical role in maintenance of cell survival in normal HSCs and myeloid progenitors such as common myeloid progenitors and GMPs through MCL-1 up-regulation.[10] In fact,

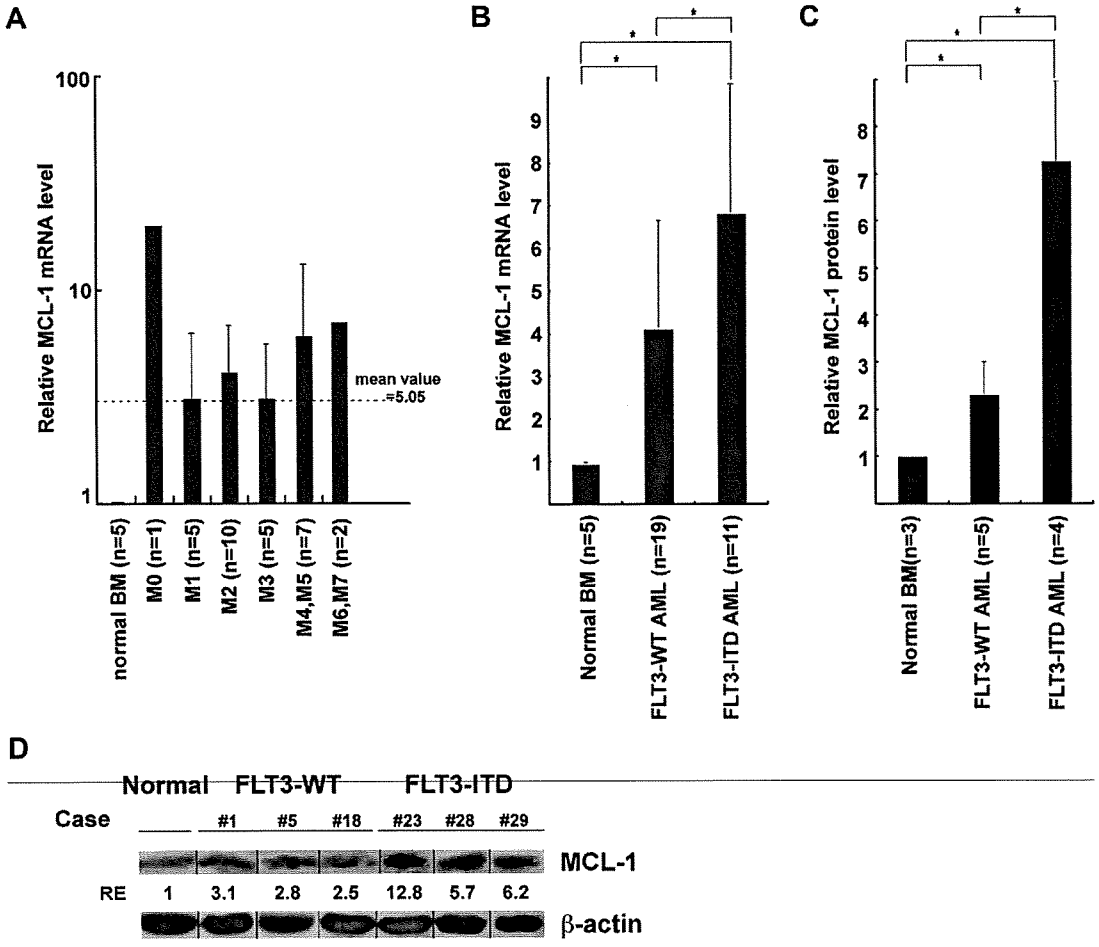

Figure 2. The expression of MCL-1 in FLT3-ITD and FLT3-WT AML cells. The levels of Mcl-1 transcripts and proteins in AML bone marrow cells. (A) AML cells express ~ 5-fold higher levels of MCL-1 compared with normal BM cells irrespective of their FAB types by real-time PCR assays. (B) FLT3-ITD AML cells expressed ~ 2-fold higher levels of MCL-1 in average compared with those in FLT3-WT AML cells. (C) The level of MCL-1 protein on Western blot analysis in primary AML cells. Results are shown as mean ± SD (*$P < .05$). (D) Representative Western blot data of MCL-1 in FLT3-WT AML (cases 1, 5, and 8) and FLT3-ITD AML (cases 23, 28, and 29) samples. Vertical lines have been inserted to indicate a repositioned gel lane.

both FLT3 and c-KIT were expressed in the $CD34^+CD38^-$ LSC fraction, and their expression levels appear to be equal in FLT3-ITD and FLT3-WT AMLs (Figure 1). We thus tested whether ligation of FLT3 and c-KIT receptors can induce further up-regulation of MCL-1 in AML LSCs in 5 cases each of FLT3-WT and FLT3-ITD AMLs. As shown in Figure 3C, both FLT3 ligand and SCF, a ligand for c-KIT, significantly up-regulated MCL-1 in LSCs. This effect was observed in both FLT3-WT and FLT3-ITD AMLs. In contrast, BCL-2 or BCL-xL expression was not significantly changed (not shown). A combination of FLT3 ligand and SCF did not show further additive effects on MCL-1 levels on LSCs (not shown). These data strongly suggest that signals of tyrosine kinase receptor family such as FLT3 and c-KIT can stimulate MCL-1 transcription in AML LSCs, presumably to prevent their apoptotic cell death.

MCL-1 is required for FLT3-ITD leukemic cells to maintain cell viability

Leukemic cell lines with FLT3-ITD, such as MV4-11, were used to analyze antiapoptotic functions of FLT3-ITD. The level of MCL-1 transcripts and proteins in MV4-11 cells was higher than that in normal BM controls, or other cell lines without FLT3 mutations such as NB4, HL-60, and U937 (Figure 4A), suggesting that FLT3-ITD signals up-regulate MCL-1 expression. MV4-11 was then treated with the tyrosine kinase inhibitor, PKC-412. PKC-412 down-regulated the expression of MCL-1 protein in a dose-dependent fashion (Figure 4B top). At the concentration of 0.5μM, MCL-1 was progressively inhibited (Figure 4B top), and reached plateau at 48 hours (not shown). PKC-412 induced apoptotic cell death of MV4-11 cells 24 hours after initiation of culture in a dose-dependent manner (Figure 4B bottom).

We then tested whether reinforcement of MCL-1 can rescue FLT3-ITD cells from PKC-412–induced apoptosis. Expression vectors harboring MCL-1–enhanced green fluorescent protein and control EGFP were transduced into these FLT3-ITD AML cell lines. Forty-eight hours after transduction, an amount of MCL-1 mRNA in FLT3-ITD–$EGFP^+$ cells was increased up to approximately 3-fold compared with those with a control vector (Figure 4C left). A significant increase in MCL-1 protein was also observed after transduction of MCL-1–EGFP vector (Figure 4C left). Purified FLT3-ITD–$EGFP^+$ cells were incubated with graded concentrations of PKC-412 for 24 hours. PKC-412–induced apoptosis was significantly inhibited in cells transduced with MCL-1 transgene (Figure 4C right; supplemental Figure 1A, available on the *Blood* website; see the Supplemental Materials link at the top of the online article), suggesting that maintenance of MCL-1 level is critical for cell survival under this condition. We then inhibited MCL-1 expression in FLT3-ITD AML cell lines by transducing an

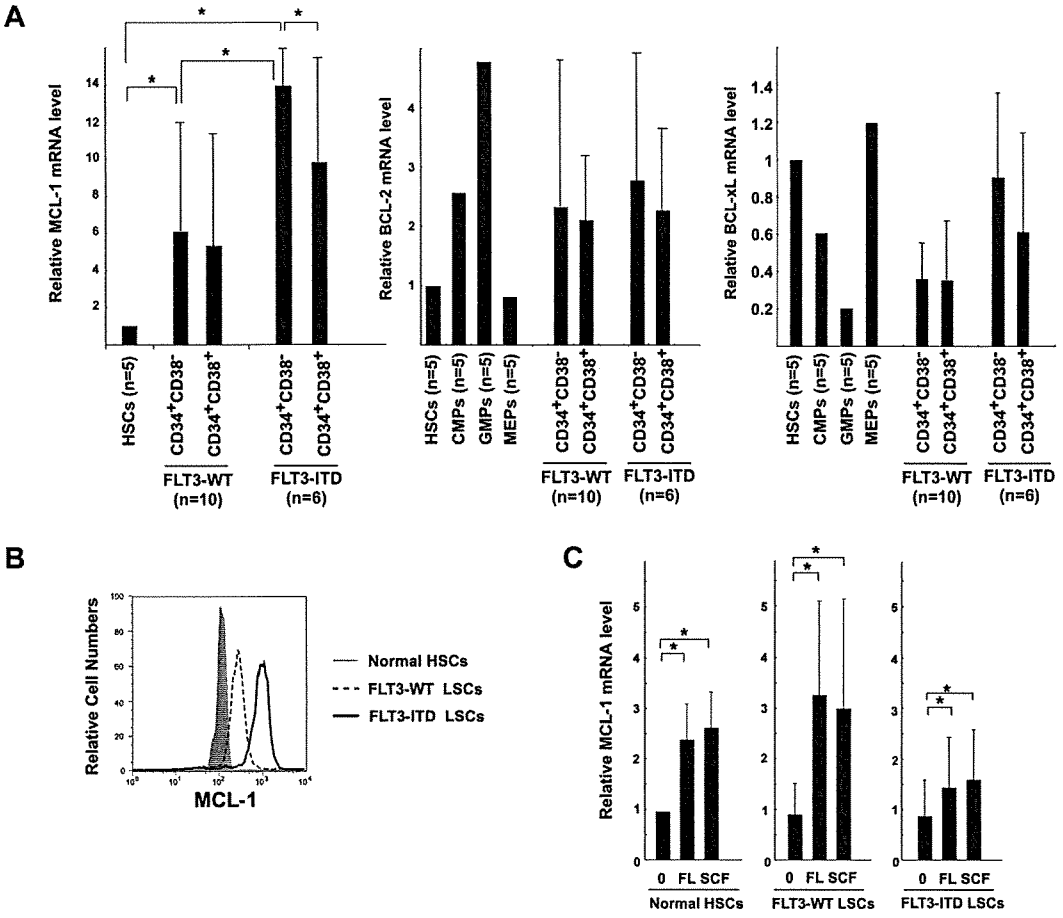

Figure 3. MCL-1 expression and its regulation in AML LSCs. (A) Real-time PCR analysis of MCL-1, BCL-2, and BCL-xl expression within fractions of $CD34^+$ cells. The LSC-enriched $CD34^+CD38^-$ fraction in FLT3-WT AML (cases 1, 3-5, 8-10, 16, 18, and 19) expressed Mcl-1 at a level > 6-fold higher than that of normal HSCs, whereas LSCs in FLT3-ITD AML (cases 20, 22-24, 27, and 30) expressed even ~ 2-fold higher levels of MCL-1 compared with FLT3-WT LSCs. In contrast, BCL-2 or BCL-xL expression was not significantly changed. (B) Cytoplasmic staining of MCL-1 in $CD34^+CD38^-$ AML fractions with FLT3-ITD and FLT3-WT. A high amount of MCL-1 protein is detectable in FLT3-ITD LSCs. Representative FLT3-ITD and FLT3-WT LSCs are shown. (C) Changes in the expression level of MCL-1 in normal HSCs, LSCs of FLT3-WT AML, and of FLT3-ITD AML after incubation with FL or with SCF. Each bar represents an n-fold difference in the amount of MCL-1 expression prior to stimulation of normal HSCs. Results are mean ± SD (*$P < .05$).

shRNA expression vector. Vectors having MCL-1–shRNA–EGFP or control EGFP were transduced and the sorted live cells ($EGFP^+$) were analyzed at 48 hours (Figure 4D). The amount of MCL-1 transcript reduced to approximately 60% of a control level. MCL-1 protein expression was also significantly reduced on FACS and Western blot analyses (Figure 4D middle). In parallel, numbers of apoptotic cells within MCL-1–shRNA–$EGFP^+$ cells were increased up to approximately 2-fold compared with those in a control (Figure 4D right; supplemental Figure 1B). These results collectively suggest that FLT3-ITD supports leukemic cell survival by up-regulating MCL-1 production.

Enforced expression of FLT3-ITD stimulates MCL-1 expression in HSCs via the STAT5-dependent signaling pathway

To confirm that FLT3-ITD signals up-regulate MCL-1 expression, we transduced FLT3-ITD into purified murine HSCs and myeloid progenitors. Cells were purified from C57BL6/Ka-Thy1.1 mice and were infected with retrovirus vectors with FLT3-ITD-GFP or FLT3-WT-GFP constructs. Thirty-six hours after retroviral transduction, GFP^+ cells were purified, and MCL-1 transcripts were quantified. In transducing retroviruses, we cultured cells with SCF, leukemia inhibitory factor, and FL, and these factors themselves have potential to stimulate MCL-1 expression.[9] In fact, control HSCs infected with the empty vector up-regulated MCL-1 mRNA up to 4-fold after this treatment (not shown). HSCs transduced with FLT3-WT expressed an amount of MCL-1 transcript almost equal to HSCs with an empty vector, suggesting that HSCs with retroviral transduction have up-regulated MCL-1 expression presumably via normal FLT3 and c-KIT signaling during cultures. In contrast, HSCs transduced with FLT3-ITD further up-regulated MCL-1 expression at a level approximately 9-fold higher than those of HSCs infected with control or FLT3-WT retroviruses (Figure 5A). BCL-2 and BCL-xL mRNA levels were not significantly changed by this treatment (not shown). The up-regulation of MCL-1 transcripts by FLT3-ITD transduction was also seen in GMPs, but the effect was less significant compared with that in HSCs, suggesting that HSCs are the favorable target for FLT3-ITD signals to up-regulate MCL-1 transcripts. Importantly, because FLT3-ITD further stimulated MCL-1 expression in the presence of normal c-KIT and FLT3 signaling, it is suggested that a novel signaling cascade independent of the pathways induced by wild-type tyrosine kinase receptors should operate to up-regulate MCL-1 expression in HSCs transduced with FLT3-ITD (Figure 5A). Previous reports have shown that FLT3-ITD possessed 2 STAT5-docking domains, whereas FLT3-WT does not.[27,43-45] We have shown that activation of STAT5 is necessary for FLT3-ITD to induce myeloproliferation,

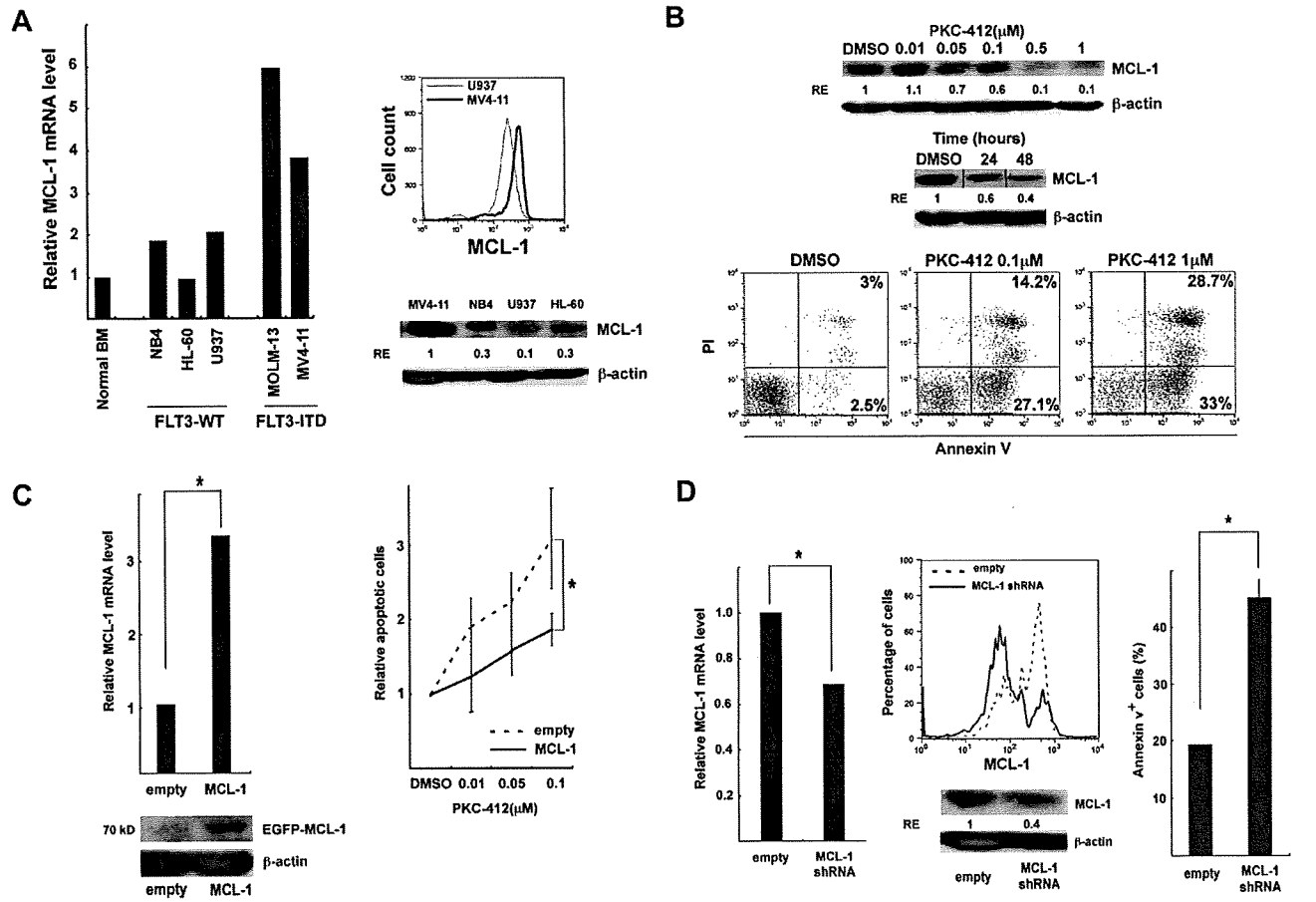

Figure 4. Functional analysis of MCL-1 in FLT3-ITD AML. (A) MCL-1 expression in cell lines with FLT3-WT (NB4, HL-60, U937) and FLT3-ITD (MV4-11 and MOLM-13). High levels of MCL-1 mRNA and protein were seen in MV4-11 cells by real-time PCR analysis (left panel), the intracellular MCL-1 staining, and Western blot analysis (right panels). (B) The inhibition of MCL-1 protein (top) and cell survival (bottom) in MV4-11 after PKC-412 treatment. The inhibitory effect of PKC-412 reached plateau at a concentration of 0.5μM. Apoptotic cell death was evaluated by annexin/PI staining. Vertical lines have been inserted to indicate a repositioned gel lane. (C) The enforced expression of MCL-1 prevented FLT3-ITD cell lines from apoptosis in the presence of PKC-412. MCL-1 transcript and protein expression were significantly up-regulated 48 hours after transduction of MCL-1 into MV4-11 cells. PKC-412–induced apoptotic cell death is significantly inhibited in MV4-11 cells (right panel) (*$P < .05$). (D) Inhibition of MCL-1 by shRNA resulted in an apoptosis of FLT3-ITD cell lines. Forty-eight hours after transduction of MCL-1–shRNA–EGFP into the MV4-11 cells, MCL-1 transcript (left) as well as MCL-1 protein expression on FACS and Western blot analysis (middle) was significantly down-regulated. In parallel, the number of apoptotic cells increased by ~ 2-fold compared with control (right). Results are shown as mean ± SD (*$P < .05$). RE indicates relative expression levels.

because transfection of the FLT3-ITD–Y589/591F mutant, in which tyrosine residues 589 and 591 located in each of these STAT5-docking sites (Figure 5B) were substituted by phenylalanine, could not induce myeloproliferative disorder in a mouse model.[30] We therefore hypothesized that the FLT3-ITD–specific MCL-1 activation might occur via its STAT5-docking domains. As shown in Figure 5A, up-regulation of MCL-1 transcripts is completely abrogated by transducing the FLT3-ITD–Y589/591F mutant instead of FLT3-ITD.

To directly test whether STAT5 is necessary in FLT3-ITD–induced MCL-1 expression, we knocked down the expression of STAT5 by transducing STAT5 siRNA into FLT3-ITD MV4-11 cells (Figure 5C). Under these conditions, MCL-1 expression was significantly inhibited at both mRNA and protein levels, suggesting that STAT5 is critical for MCL-1 expression. Figure 5B schematizes the FLT3-ITD and FLT3 signaling pathways for MCL-1 expression. In FLT3-WT, FLT3 ligation triggers both PI3K/Akt and RAS/MEK/MAPK pathways.[23] In FLT3-ITD cells, FLT3-ITD might directly activate STAT5 via its STAT5-docking sites. Treatment of MV4-11 cells with AG290, a Janus kinase 2 (JAK2) inhibitor, did not affect MCL-1 expression (Figure 5D). Thus, activated STAT5 triggers MCL-1 transcription without JAK2 activation. We then tried to test whether STAT5 induces MCL-1 expression by triggering activation of the PI3K/Akt pathway: Ly294002, a PI3K inhibitor, did not affect MCL-1 mRNA expression but significantly inhibited MCL-1 protein expression (Figure 5D), suggesting that the PI3K pathway regulates MCL-1 expression at the protein level. Of note, STAT5 inhibition significantly down-regulated the phosphorylation of Akt, a downstream molecule of PI3K, indicating that STAT5 is positioned upstream of the PI3K pathway (Figure 5C). On the other hand, STAT5 siRNA did not affect MEK phosphorylation (Figure 5C), and U0126, a MEK inhibitor, did not change the expression of either MCL-1 mRNA or protein (Figure 5D), suggesting that STAT5-induced MCL-1 expression is not mediated by the RAS/MEK/MAPK pathway. Collectively, in FLT3-ITD signaling pathway, STAT5 up-regulates MCL-1 by triggering MCL-1 transcription, and by activating PI3K to posttranscriptionally up-regulate MCL-1.

Discussion

FLT3 mutations are among the most common genetic alterations in AML. FLT3-ITD results in loss of function of a juxtamembrane autoinhibitory domain that maintains the kinase in an inactive state in the absence of ligand, resulting in ligand-independent receptor

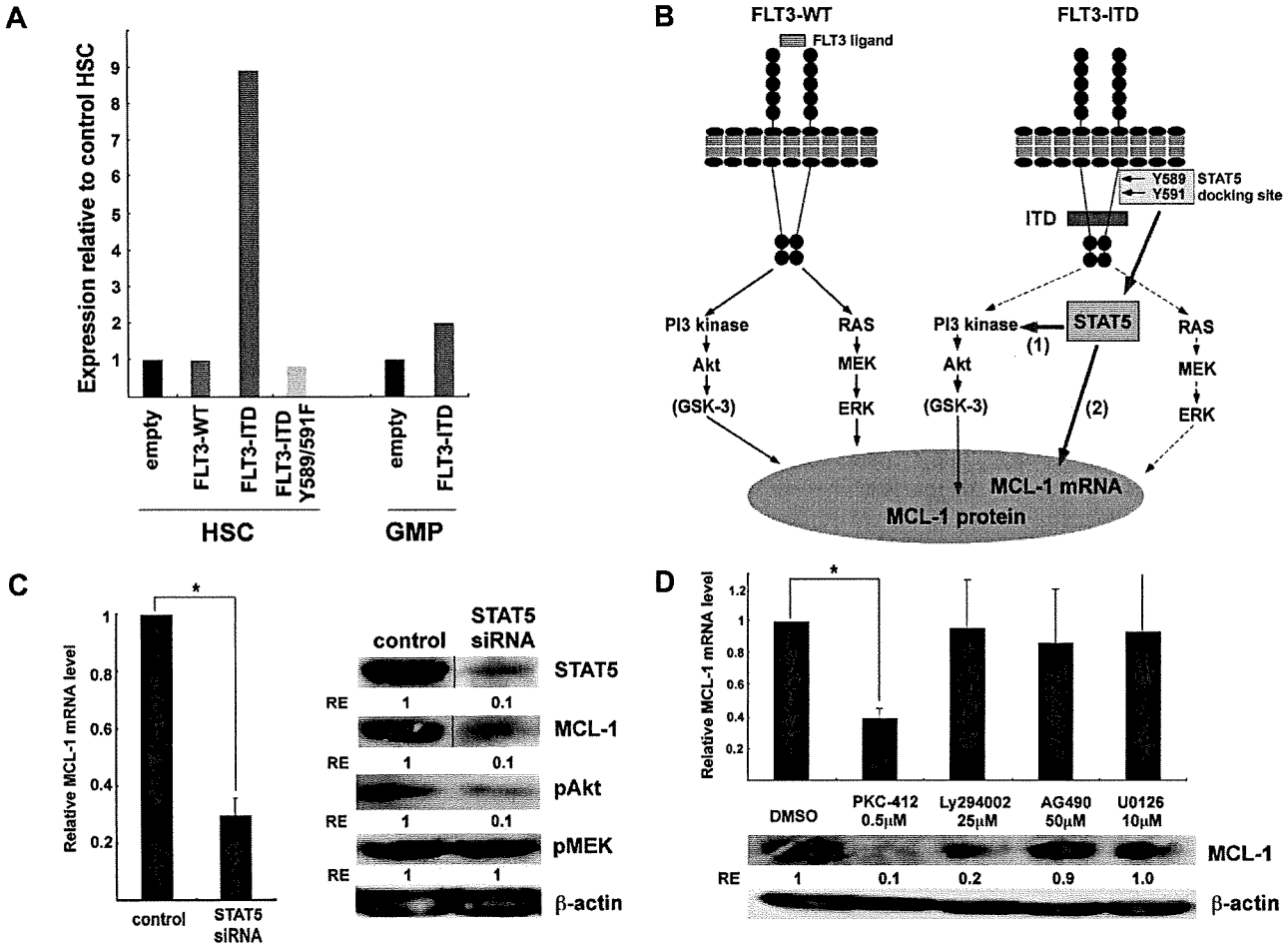

Figure 5. FLT3-ITD activates MCL-1 expression via STAT5 signaling. (A) FLT3-WT, FLT3-ITD, and FLT3-ITD-Y589/591F mutants were transduced into purified murine HSCs and GMPs to test changes in the amount of MCL-1 transcripts. During the transduction, cells were cultured for 48 hours in the presence of FLT3 and SCF. In this condition, the amount of MCL-1 transcripts in HSCs transfected with FLT3-WT was almost equal to HSCs with an empty vector. Significant up-regulation of MCL-1 (~ 9-fold higher) was seen when HSCs were transfected with FLT3-ITD. This effect was more pronounced in HSCs than GMPs. The up-regulation of MCL-1 was completely inhibited in HSCs transduced with FLT3-ITD-Y589/591F mutant, indicating that FLT3-ITD–specific STAT5-docking phosphorylation sites are necessary to stimulate MCL-1 transcription. (B) Schematic presentation of signaling pathways of FLT3-ITD to induce MCL-1 expression. In FLT3-WT, FLT3 ligation triggers both PI3K/Akt and RAS/MAPK pathways. In contrast, FLT3-ITD induces STAT5-dependent MCL-1 expression. STAT5 might induce MCL-1 expression by PI3K/Akt activation presumably through posttranscriptional mechanism (1), and by directly stimulating MCL-1 transcription (2). These 2 distinct FLT3-ITD signaling pathways for MCL-1 expression contribute to the development of AML. (C) STAT5 siRNA was transduced into MV4-11 cell lines to suppress STAT5 expression. The sorted live cells were analyzed at 48 hours after STAT5 siRNA transduction. STAT5 siRNA suppressed the expression of MCL-1 transcript and protein. STAT5 siRNA also suppressed phospho-Akt, but not phospho-MEK, pathway. Vertical lines have been inserted to indicate a repositioned gel lane. Results are shown as mean ± SD (*$P < .05$) (D) The expression of MCL-1 in MV4-11 24 hours after treatment with pharmacologic inhibitors of PKC (PKC-412), PI3K (Ly294002), JAK2 (AG490), or MEK (U0126). PKC-412 inhibited MCL-1 mRNA expression. PKC-412 and Ly294002 but not U0126 or AG490 inhibited the MCL-1 protein expression. RE indicates relative expression levels. Results are shown as mean ± SD (*$P < .05$).

dimerization and constitutive FLT3 signaling. In addition to the normal FLT3 signaling, including activation of the RAS/MAPK and PI3K pathways, FLT3-ITD can activate STAT5 via FLT3-ITD–specific STAT5-docking domains. In a mouse line harboring FLT3-ITD knocked into the *Flt3* locus, bone marrow cells displayed myeloproliferation resembling the phenotype of chronic myelomonocytic leukemia. Because this finding correlated at least with an increase in number and survival of multipotent progenitors,[46] the reinforcement of cell survival might be one of the critical roles of FLT3-ITD.

The $CD34^+CD38^-$ LSCs purified from FLT3-ITD AML patients can repopulate the disease in the immune-deficient mice after transplantation, confirming that FLT3-ITD mutations are acquired at the LSC level.[47] We here show that the extracellular FLT3 is expressed at a high level in LSCs on FACS in all types of human AML irrespective of the presence of FLT3-ITD mutations. Because anti-FLT3 antibodies should react with FLT3-ITD, both FLT3 and FLT3-ITD are expressed in AML LSCs at a high level (Figure 1), suggesting that FLT3-ITD signaling should operate strongly at the LSC stage in AML. In normal human HSCs, FLT3 signaling is critical for maintenance of MCL-1 at a high level.[10] Of note, freshly isolated AML LSCs express a higher level of FLT3 and MCL-1 compared with normal HSCs, which may lead to growth advantages of AML LSCs against normal HSCs in vivo. The high level of MCL-1 in purified AML LSCs (Figure 3A) may be derived from signals from a higher amount of FLT3 on LSCs' surface (Figure 1). The ligation of their FLT3 receptors induced even higher levels of MCL-1 in LSCs (Figure 3C). Freshly isolated FLT3-ITD LSCs already maintained a high level of MCL-1, but an addition of FLT3 ligand could cause further up-regulation of MCL-1 (Figure 3C). This additive effect could be due to ligation of normal FLT3 receptors generated from an intact FLT3 allele.

One of the major functions of FLT3-ITD signaling should prevent LSCs from apoptotic cell death via maintaining a high level of MCL-1, as directly shown in Figure 4. It has recently been demonstrated that the ratio of FLT3-ITD/WT mRNA expression

shows a wide variation in the samples of AML blasts.[21,48] Of note, higher FLT3-ITD/WT ratio manifests significantly shorter overall and disease-free survival of patients.[21,48,49] We thus investigated the association between the ratio of FLT3-ITD/WT transcripts and MCL-1 expression in our AML samples. This ratio, however, did not correlate with the levels of MCL-1 expression in the samples analyzed so far (data not shown). Due to limited number of samples, further experiments are still needed to address this issue.

Our study also showed that the FLT3-ITD–specific STAT5-docking domains play a major role for FLT3-ITD, independent of JAK2 activation, to induce MCL-1 mRNA (Figure 5). This is of particular interest because these domains are necessary to cause myeloproliferative phenotype in a FLT3-ITD knock-in strain.[46] STAT5 is well recognized as a common downstream pathway from cytokine receptors, and activates transcription of various target genes such as cyclin D1, p21, Pim-1, c-fos, and BCL-xL.[46,50] Sustained activation of STAT5 in murine HSCs but not progenitors induced myeloproliferative disease, and knockdown of STAT5 impaired growth of normal and leukemic stem cells, indicating that STAT5 plays a crucial role in proliferation or survival of HSCs and LSCs.[51,52] It has also been reported that AML cells with STAT5 phosphorylation display a lower percentage of spontaneous apoptosis, compared with AML cells without STAT5 phosphorylation, and constitutive STAT5 phosphorylation was observed with all AML cases with FLT3-ITD.[44] Furthermore, AG1296, a tyrosine kinase inhibitor, strongly inhibited STAT5 phosphorylation and induced apoptosis in AML cells.[44] In this study, we show that STAT5 is particularly critical for FLT3-ITD signaling to express MCL-1, because knockdown of STAT5 abrogates MCL-1 expression in FLT3-ITD cells at both mRNA and protein levels (Figure 5C). Of note, the STAT-binding motif is found in the promoter of the human *MCL-1* gene,[53] suggesting that STAT5 could directly activate the transcription of *MCL-1* gene. Previous studies including our own have shown that MCL-1 expression is regulated also at the protein level by the PI3K pathway, because Akt, a downstream molecule of PI3K, up-regulates MCL-1 posttranscriptionally via regulating activation of glycogen synthase kinase 3.[54,55] Interestingly, recent studies have shown that STAT5 interacts with and activates PI3K.[56,57] We found that STAT5 knockdown inhibits phosphorylation of Akt and suppresses MCL-1 expression in FLT3-ITD cells (Figure 5C). It is thus likely that STAT5 could also activate the PI3K/Akt pathway to up-regulate MCL-1 at the protein level. Therefore, the STAT5/MCL-1 pathway downstream of FLT3-ITD could be a specific target to impair survival of FLT3-ITD LSCs, still sparing the effect on FLT3-dependent normal hematopoiesis.

The reinforcement of survival is one of the critical factors for leukemia development. We have reported that the myeloproliferative phenotype develops also in a mouse model expressing simply a Bcl-2 transgene at the myeloid progenitor stage using the myeloid-related protein-8 promoter.[7] Furthermore, the myeloid-related protein-8–BCL-2 transgene accelerates the AML development in mice having leukemogenic mutations such as BCR-ABL[7] and promyelocytic leukemia/retinoic acid receptor α (PML/RARα).[6] Previous studies have shown that FLT3 mutations alone are not sufficient to cause AML, and that additional cooperating mutations are required for AML development.[23,24] When FLT3-ITDs are combined with other genetic alterations such as PML-RARα,[58] AML1-ETO,[59] MLL-AF9,[60] and NUP98-HOX,[61] full transformation to AML can occur. Our data suggest that the primary role of FLT3-ITD in AML is at least to reinforce cell survival to promote AML development.

Thus, the $CD34^+CD38^-$ AML fraction that concentrates LSCs possesses a high level of MCL-1 and might use this protein to ensure their survival. The acquisition of FLT3-ITD mutation provides LSCs with potent survival signals through further up-regulating MCL-1. This survival-promoting signal of FLT3-ITD is mediated by a STAT5-dependent pathway that is independent of normal FLT3 signaling. Targeting this pathway might be useful to trigger cell death process specifically in FLT3-ITD AML LSCs.

Acknowledgments

We appreciate the medical and nursing staff working on the Fukuoka Blood and Marrow Transplantation Group.

This work was supported in part by a Grant-in-Aid from the Ministry of Education, Culture, Sports, Science and Technology in Japan (19659248 and 20390272 [T.M.], 17109010 and 17047029 [K.A.]) and the Takeda Science Foundation (T.M.).

Authorship

Contribution: G.Y., T.M., and K.A. designed and performed research, analyzed data, and wrote the paper; S.J.-T., T.I., Y.K., Y.M., T.S., H.N., and S.-i.M. performed research; H.I., K.T., and K.N. provided patients' samples and information; and J.L.R. and G.D.G. provided cDNA constructs and helped to write the manuscript.

Conflict-of-interest disclosure: The authors declare no competing financial interests.

Correspondence: Koichi Akashi, Department of Medicine and Biosystemic Science, Graduate School of Medical Sciences, Kyushu University, 3-1-1 Maidashi, Higashi-ku, Fukuoka 812-8582, Japan; e-mail: akashi@med.kyushu-u.ac.jp.

References

1. Hanahan D, Weinberg RA. The hallmarks of cancer. *Cell.* 2000;100(1):57-70.
2. Green DR, Evan GI. A matter of life and death. *Cancer Cell.* 2002;1(1):19-30.
3. Cory S, Huang DC, Adams JM. The Bcl-2 family: roles in cell survival and oncogenesis. *Oncogene.* 2003;22(53):8590-8607.
4. Danial NN, Korsmeyer SJ. Cell death: critical control points. *Cell.* 2004;116(2):205-219.
5. Traver D, Akashi K, Weissman IL, Lagasse E. Mice defective in two apoptosis pathways in the myeloid lineage develop acute myeloblastic leukemia. *Immunity.* 1998;9(1):47-57.
6. Kogan SC, Brown DE, Shultz DB, et al. BCL-2 cooperates with promyelocytic leukemia retinoic acid receptor alpha chimeric protein (PMLRARalpha) to block neutrophil differentiation and initiate acute leukemia. *J Exp Med.* 2001;193(4):531-543.
7. Jaiswal S, Traver D, Miyamoto T, Akashi K, Lagasse E, Weissman IL. Expression of BCR/ABL and BCL-2 in myeloid progenitors leads to myeloid leukemias. *Proc Natl Acad Sci U S A.* 2003;100(17):10002-10007.
8. Kozopas KM, Yang T, Buchan HL, Zhou P, Craig RW. MCL1, a gene expressed in programmed myeloid cell differentiation, has sequence similarity to BCL2. *Proc Natl Acad Sci U S A.* 1993;90(8):3516-3520.
9. Opferman JT, Iwasaki H, Ong CC, et al. Obligate role of anti-apoptotic MCL-1 in the survival of hematopoietic stem cells. *Science.* 2005;307(5712):1101-1104.
10. Kikushige Y, Yoshimoto G, Miyamoto T, et al. Human Flt3 is expressed at the hematopoietic stem cell and the granulocyte/macrophage progenitor stages to maintain cell survival. *J Immunol.* 2008;180(11):7358-7367.
11. Zhou P, Levy NB, Xie H, et al. MCL1 transgenic mice exhibit a high incidence of B-cell lymphoma manifested as a spectrum of histologic subtypes. *Blood.* 2001;97(12):3902-3909.
12. Jourdan M, Veyrune JL, De Vos J, Redal N, Couderc G, Klein B. A major role for Mcl-1 antiapoptotic protein in the IL-6-induced survival of human myeloma cells. *Oncogene.* 2003;22(19):2950-2959.

13. Kitada S, Reed JC. MCL-1 promoter insertions dial-up aggressiveness of chronic leukemia. *J Natl Cancer Inst.* 2004;96(9):642-643.
14. Petlickovski A, Laurenti L, Li X, et al. Sustained signaling through the B-cell receptor induces Mcl-1 and promotes survival of chronic lymphocytic leukemia B cells. *Blood.* 2005;105(12):4820-4827.
15. Kitada S, Andersen J, Akar S, et al. Expression of apoptosis-regulating proteins in chronic lymphocytic leukemia: correlations with In vitro and In vivo chemoresponses. *Blood.* 1998;91(9):3379-3389.
16. Derenne S, Monia B, Dean NM, et al. Antisense strategy shows that Mcl-1 rather than Bcl-2 or Bcl-x(L) is an essential survival protein of human myeloma cells. *Blood.* 2002;100(1):194-199.
17. Hannum C, Culpepper J, Campbell D, et al. Ligand for FLT3/FLK2 receptor tyrosine kinase regulates growth of haematopoietic stem cells and is encoded by variant RNAs. *Nature.* 1994; 368(6472):643-648.
18. Carow CE, Levenstein M, Kaufmann SH, et al. Expression of the hematopoietic growth factor receptor FLT3 (STK-1/Flk2) in human leukemias. *Blood.* 1996;87(3):1089-1096.
19. Nakao M, Yokota S, Iwai T, et al. Internal tandem duplication of the flt3 gene found in acute myeloid leukemia. *Leukemia.* 1996;10(12):1911-1918.
20. Kiyoi H, Naoe T, Nakano Y, et al. Prognostic implication of FLT3 and N-RAS gene mutations in acute myeloid leukemia. *Blood.* 1999;93(9):3074-3080.
21. Thiede C, Steudel C, Mohr B, et al. Analysis of FLT3-activating mutations in 979 patients with acute myelogenous leukemia: association with FAB subtypes and identification of subgroups with poor prognosis. *Blood.* 2002;99(12):4326-4335.
22. Schnittger S, Schoch C, Dugas M, et al. Analysis of FLT3 length mutations in 1003 patients with acute myeloid leukemia: correlation to cytogenetics, FAB subtype, and prognosis in the AMLCG study and usefulness as a marker for the detection of minimal residual disease. *Blood.* 2002; 100(1):59-66.
23. Gilliland DG, Griffin JD. The roles of FLT3 in hematopoiesis and leukemia. *Blood.* 2002;100(5): 1532-1542.
24. Kelly LM, Liu Q, Kutok JL, Williams IR, Boulton CL, Gilliland DG. FLT3 internal tandem duplication mutations associated with human acute myeloid leukemias induce myeloproliferative disease in a murine bone marrow transplant model. *Blood.* 2002;99(1):310-318.
25. Stirewalt DL, Radich JP. The role of FLT3 in haematopoietic malignancies. *Nat Rev Cancer.* 2003;3(9):650-665.
26. Kiyoi H, Towatari M, Yokota S, et al. Internal tandem duplication of the FLT3 gene is a novel modality of elongation mutation which causes constitutive activation of the product. *Leukemia.* 1998; 12(9):1333-1337.
27. Hayakawa F, Towatari M, Kiyoi H, et al. Tandem-duplicated Flt3 constitutively activates STAT5 and MAP kinase and introduces autonomous cell growth in IL-3-dependent cell lines. *Oncogene.* 2000;19(5):624-631.
28. Kiyoi H, Ohno R, Ueda R, Saito H, Naoe T. Mechanism of constitutive activation of FLT3 with internal tandem duplication in the juxtamembrane domain. *Oncogene.* 2002;21(16):2555-2563.
29. Zheng R, Friedman AD, Small D. Targeted inhibition of FLT3 overcomes the block to myeloid differentiation in 32Dcl3 cells caused by expression of FLT3/ITD mutations. *Blood.* 2002;100(12): 4154-4161.
30. Rocnik JL, Okabe R, Yu JC, et al. Roles of tyrosine 589 and 591 in STAT5 activation and transformation mediated by FLT3-ITD. *Blood.* 2006;108(4):1339-1345.
31. Yoshimoto G, Nagafuji K, Miyamoto T, et al. FLT3 mutations in normal karyotype acute myeloid leukemia in first complete remission treated with autologous peripheral blood stem cell transplantation. *Bone Marrow Transplant.* 2005;36(11):977-983.
32. Manz MG, Miyamoto T, Akashi K, Weissman IL. Prospective isolation of human clonogenic common myeloid progenitors. *Proc Natl Acad Sci U S A.* 2002;99(18):11872-11877.
33. Miyamoto T, Weissman IL, Akashi K. AML1/ETO-expressing nonleukemic stem cells in acute myelogenous leukemia with 8;21 chromosomal translocation. *Proc Natl Acad Sci U S A.* 2000; 97(13):7521-7526.
34. Iwasaki H, Somoza C, Shigematsu H, et al. Distinctive and indispensable roles of PU. 1 in maintenance of hematopoietic stem cells and their differentiation. *Blood.* 2005;106(5):1590-1600.
35. Niiro H, Maeda A, Kurosaki T, Clark EA. The B lymphocyte adaptor molecule of 32 kD (Bam32) regulates B cell antigen receptor signaling and cell survival. *J Exp Med.* 2002;195(1):143-149.
36. Baum CM, Weissman IL, Tsukamoto AS, Buckle AM, Peault B. Isolation of a candidate human hematopoietic stem-cell population. *Proc Natl Acad Sci U S A.* 1992;89(7):2804-2808.
37. Craig W, Kay R, Cutler RL, Lansdorp PM. Expression of Thy-1 on human hematopoietic progenitor cells. *J Exp Med.* 1993;177(5):1331-1342.
38. Murray L, Chen B, Galy A, et al. Enrichment of human hematopoietic stem cell activity in the CD34+Thy-1+Lin- subpopulation from mobilized peripheral blood. *Blood.* 1995;85(2):368-378.
39. Bonnet D, Dick JE. Human acute myeloid leukemia is organized as a hierarchy that originates from a primitive hematopoietic cell. *Nat Med.* 1997;3(7):730-737.
40. Ishikawa F, Yoshida S, Saito Y, et al. Chemotherapy-resistant human AML stem cells home to and engraft within the bone-marrow endosteal region. *Nat Biotechnol.* 2007;25(11):1315-1321.
41. Holden JT, Geller RB, Farhi DC, et al. Characterization of Thy-1 (CDw90) expression in CD34+ acute leukemia. *Blood.* 1995;86(1):60-65.
42. Kozii R, Wilson J, Persichetti J, Phelps V, Ball SE, Ball ED. Thy-1 expression on blast cells from adult patients with acute myeloid leukemia. *Leuk Res.* 1997;21(5):381-385.
43. Mizuki M, Fenski R, Halfter H, et al. Flt3 mutations from patients with acute myeloid leukemia induce transformation of 32D cells mediated by the Ras and STAT5 pathways. *Blood.* 2000; 96(12):3907-3914.
44. Birkenkamp KU, Geugien M, Lemmink HH, Kruijer W, Vellenga E. Regulation of constitutive STAT5 phosphorylation in acute myeloid leukemia blasts. *Leukemia.* 2001;15(12):1923-1931.
45. Spiekermann K, Bagrintseva K, Schwab R, Schmieja K, Hiddemann W. Overexpression and constitutive activation of FLT3 induces STAT5 activation in primary acute myeloid leukemia blast cells. *Clin Cancer Res.* 2003;9(6):2140-2150.
46. Lee BH, Tothova Z, Levine RL, et al. FLT3 mutations confer enhanced proliferation and survival properties to multipotent progenitors in a murine model of chronic myelomonocytic leukemia. *Cancer Cell.* 2007;12(4):367-380.
47. Levis M, Murphy KM, Pham R, et al. Internal tandem duplications of the FLT3 gene are present in leukemia stem cells. *Blood.* 2005;106(2):673-680.
48. Kottaridis PD, Gale RE, Frew ME, et al. The presence of a FLT3 internal tandem duplication in patients with acute myeloid leukemia (AML) adds important prognostic information to cytogenetic risk group and response to the first cycle of chemotherapy: analysis of 854 patients from the United Kingdom Medical Research Council AML 10 and 12 trials. *Blood.* 2001;98(6):1752-1759.
49. Whitman SP, Archer KJ, Feng L, et al. Absence of the wild-type allele predicts poor prognosis in adult de novo acute myeloid leukemia with normal cytogenetics and the internal tandem duplication of FLT3: a cancer and leukemia group B study. *Cancer Res.* 2001;61(19):7233-7239.
50. Haura EB, Turkson J, Jove R. Mechanisms of disease: insights into the emerging role of signal transducers and activators of transcription in cancer. *Nat Clin Pract Oncol.* 2005;2(6):315-324.
51. Kato Y, Iwama A, Tadokoro Y, et al. Selective activation of STAT5 unveils its role in stem cell self-renewal in normal and leukemic hematopoiesis. *J Exp Med.* 2005;202(1):169-179.
52. Schepers H, van Gosliga D, Wierenga AT, Eggen BJ, Schuringa JJ, Vellenga E. STAT5 is required for long-term maintenance of normal and leukemic human stem/progenitor cells. *Blood.* 2007; 110(8):2880-2888.
53. Akgul C, Turner PC, White MR, Edwards SW. Functional analysis of the human MCL-1 gene. *Cell Mol Life Sci.* 2000;57(4):684-691.
54. Maurer U, Charvet C, Wagman AS, Dejardin E, Green DR. Glycogen synthase kinase-3 regulates mitochondrial outer membrane permeabilization and apoptosis by destabilization of MCL-1. *Mol Cell.* 2006;21(6):749-760.
55. Tabrizi SJ, Niiro H, Masui M, et al. T cell leukemia/lymphoma 1 and galectin-1 regulate survival/cell death pathways in human naive and IgM+ memory B cells through altering balances in Bcl-2 family proteins. *J Immunol.* 2009;182(3):1490-1499.
56. Kornfeld M. Neuropathology of chronic GM2 gangliosidosis due to hexosaminidase A deficiency. *Clin Neuropathol.* 2008;27(5):302-308.
57. Harir N, Boudot C, Friedbichler K, et al. Oncogenic Kit controls neoplastic mast cell growth through a Stat5/PI3-kinase signaling cascade. *Blood.* 2008;112(6):2463-2473.
58. Kelly LM, Kutok JL, Williams IR, et al. PML/RARalpha and FLT3-ITD induce an APL-like disease in a mouse model. *Proc Natl Acad Sci U S A.* 2002;99(12):8283-8288.
59. Schessl C, Rawat VP, Cusan M, et al. The AML1-ETO fusion gene and the FLT3 length mutation collaborate in inducing acute leukemia in mice. *J Clin Invest.* 2005;115(8):2159-2168.
60. Stubbs MC, Kim YM, Krivtsov AV, et al. MLL-AF9 and FLT3 cooperation in acute myelogenous leukemia: development of a model for rapid therapeutic assessment. *Leukemia.* 2008;22(1):66-77.
61. Palmqvist L, Argiropoulos B, Pineault N, et al. The Flt3 receptor tyrosine kinase collaborates with NUP98-HOX fusions in acute myeloid leukemia. *Blood.* 2006;108(3):1030-1036.

blood

2009 113: 5041-5048
Prepublished online Sep 22, 2008;
doi:10.1182/blood-2008-07-171678

HapMap scanning of novel human minor histocompatibility antigens

Michi Kamei, Yasuhito Nannya, Hiroki Torikai, Takakazu Kawase, Kenjiro Taura, Yoshihiro Inamoto, Taro Takahashi, Makoto Yazaki, Satoko Morishima, Kunio Tsujimura, Koichi Miyamura, Tetsuya Ito, Hajime Togari, Stanley R. Riddell, Yoshihisa Kodera, Yasuo Morishima, Toshitada Takahashi, Kiyotaka Kuzushima, Seishi Ogawa and Yoshiki Akatsuka

Blood (print ISSN 0006-4971, online ISSN 1528-0020), is published semimonthly by the American Society of Hematology, 1900 M St, NW, Suite 200, Washington DC 20036.

HapMap scanning of novel human minor histocompatibility antigens

*Michi Kamei,[1,2] *Yasuhito Nannya,[3-5] Hiroki Torikai,[1] Takakazu Kawase,[1,6] Kenjiro Taura,[7] Yoshihiro Inamoto,[8] Taro Takahashi,[8] Makoto Yazaki,[9] Satoko Morishima,[1] Kunio Tsujimura,[10] Koichi Miyamura,[5,8] Tetsuya Ito,[2] Hajime Togari,[2] Stanley R. Riddell,[11] Yoshihisa Kodera,[5,8] Yasuo Morishima,[5,12] Toshitada Takahashi,[13] Kiyotaka Kuzushima,[1] †Seishi Ogawa,[4,5] and †Yoshiki Akatsuka[1,5]

[1]Division of Immunology, Aichi Cancer Center Research Institute, Nagoya, Japan; [2]Department of Pediatrics and Neonatology, Nagoya City University, Graduate School of Medical Science, Nagoya, Japan; [3]Department of Hematology/Oncology and [4]The 21st Century Center of Excellence (COE) Program, Graduate School of Medicine, University of Tokyo, Tokyo, Japan; [5]Core Research for Evolutional Science and Technology, Japan Science and Technology Agency, Saitama, Japan; [6]Division of Epidemiology and Prevention, Aichi Cancer Center Research Institute, Nagoya, Japan; [7]Department of Information and Communication Engineering, Graduate School of Information Science, University of Tokyo, Tokyo, Japan; [8]Department of Hematology, Japanese Red Cross Nagoya First Hospital, Nagoya, Japan; [9]Department of Pediatrics, Higashi Municipal Hospital of Nagoya, Nagoya, Japan; [10]Department of Infectious Diseases, Hamamatsu University School of Medicine, Hamamatsu, Japan; [11]Program in Immunology, Clinical Research Division, Fred Hutchinson Cancer Research Center, Seattle, WA; [12]Department of Hematology and Cell Therapy, Aichi Cancer Center Central Hospital, Nagoya, Japan; and [13]Aichi Comprehensive Health Science Center, Aichi Health Promotion Foundation, Chita-gun, Japan

Minor histocompatibility antigens (mHags) are molecular targets of alloimmunity associated with hematopoietic stem cell transplantation (HSCT) and involved in graft-versus-host disease, but they also have beneficial antitumor activity. mHags are typically defined by host SNPs that are not shared by the donor and are immunologically recognized by cytotoxic T cells isolated from post-HSCT patients. However, the number of molecularly identified mHags is still too small to allow prospective studies of their clinical importance in transplantation medicine, mostly due to the lack of an efficient method for isolation. Here we show that when combined with conventional immunologic assays, the large data set from the International HapMap Project can be directly used for genetic mapping of novel mHags. Based on the immunologically determined mHag status in HapMap panels, a target mHag locus can be uniquely mapped through whole genome association scanning taking advantage of the unprecedented resolution and power obtained with more than 3 000 000 markers. The feasibility of our approach could be supported by extensive simulations and further confirmed by actually isolating 2 novel mHags as well as 1 previously identified example. The HapMap data set represents an invaluable resource for investigating human variation, with obvious applications in genetic mapping of clinically relevant human traits. (Blood. 2009;113:5041-5048)

Introduction

The antitumor activity of allogeneic hematopoietic stem cell transplantation (HSCT), which is a curative treatment for many patients with hematologic malignancies, is mediated in part by immune responses that are elicited as a consequence of incompatibility in genetic polymorphisms between the donor and the recipient.[1,2] Analysis of patients treated for posttransplantation relapse with donor lymphocytes has shown tumor regression to be correlated with expansion of cytotoxic T lymphocytes (CTLs) specific for hematopoiesis-restricted minor histocompatibility antigens (mHags).[3,4] mHags are peptides, presented by major histocompatibility complex (MHC) molecules, derived from intracellular proteins that differ between donor and recipient due mostly to single nucleotide polymorphisms (SNPs) or copy number variations (CNVs).[1,2,5] Identification and characterization of mHags that are specifically expressed in hematopoietic but not in other normal tissues could contribute to graft-versus-leukemia/lymphoma (GVL) effects, while minimizing unfavorable graft-versus-host disease, one of the most serious complications of allo-HSCT.[1,2] Unfortunately, however, efforts to prospectively target mHags to invoke T cell–mediated selective GVL effects have been hampered by the scarcity of eligible mHags, largely due to the lack of efficient methods for mapping the relevant genetic loci. Several methods have been developed to identify mHags, including peptide elution from MHC,[6,7] cDNA expression cloning,[8,9] and linkage analysis.[3,10] We have recently reported a novel genetic method that combines whole genome association scanning with conventional chromium release cytotoxicity assays (CRAs). With this approach the genetic loci of the mHag gene recognized by a given CTL clone can be precisely identified using SNP array analysis of pooled DNA generated from immortalized lymphoblastoid cell lines (LCLs) that are immunophenotyped into $mHag^+$ and $mHag^-$ groups by CRA.[11] The mapping resolution has now been improved from several Mb for conventional linkage analysis to an average haplotype block size of less than 100 kb,[12] usually containing a handful of candidate genes. Nevertheless, it still requires laborious DNA pooling and scanning of SNP arrays with professional expertise for individual

Submitted July 29, 2008; accepted August 27, 2008. Prepublished online as *Blood* First Editon paper, September 22, 2008; DOI 10.1182/blood-2008-07-171678.

*M.K. and Y.N. are first coauthors and contributed equally to this work.

†S.O. and Y.A. are senior coauthors.

An Inside *Blood* analysis of this article appears at the front of this issue.

The online version of this article contains a data supplement.

The publication costs of this article were defrayed in part by page charge payment. Therefore, and solely to indicate this fact, this article is hereby marked "advertisement" in accordance with 18 USC section 1734.

CTLs.[11] To circumvent these drawbacks, we have sought to take advantage of publicly available HapMap resources. Here, we describe a powerful approach for rapidly identifying mHAg loci using a large genotyping data set and LCLs from the International HapMap Project for genome-wide association analysis.[13-15]

Methods

Cell lines and CTL clones

The HapMap LCL samples were purchased from the Coriell Institute (Camden, NJ). All LCLs were maintained in RPMI1640 supplemented with 10% fetal calf serum, 2 mM L-glutamine, and 1 mM sodium pyruvate. Because the recognition of a mHag requires presentation on a particular type of HLA molecule, the LCLs were stably transduced with a retroviral vector encoding the restriction HLA cDNA for a given CTL clone when necessary.[16]

CTL lines were generated from recipient peripheral blood mononuclear cells obtained after transplantation by stimulation with those harvested before HSCT after irradiation (33 Gy), and thereafter stimulated weekly in RPMI 1640 supplemented with 10% pooled human serum and 2 mM L-glutamine. Recombinant human inerleukin-2 was added on days 1 and 5 after the second and third stimulations. CTL clones were isolated by standard limiting dilution and expanded as previously described.[10,17] HLA restriction was determined by conventional CRAs against a panel of LCLs sharing HLA alleles with the CTLs. All clinical samples were collected based on a protocol approved by the Institutional Review Board Committee at Aichi Cancer Center and the University of Tokyoand after written informed consent was obtained in accordance with the Declaration of Helsinki.

Immunophenotyping of HapMap LCLs and high-density genome-wide scanning of mHag loci

Case ($mHag^+$) - control ($mHag^-$) LCL panels were generated by screening corresponding restriction HLA-transduced CHB and JPT HapMap LCL panels with each CTL clone using CRAs. Briefly, target cells were labeled with 0.1 mCi of ^{51}Cr for 2 hours, and 10^3 target cells per well were mixed with CTL at a predetermined E/T ratio in a standard 4-hour CRA. All assays were performed at least in duplicate. The percent specific lysis was calculated by ((Experimental cpm - Spontaneous cpm) / (Maximum cpm - Spontaneous cpm)) × 100. After normalization by dividing their percent specific lysis values by that of positive control LCL (typically recipient-derived LCL corresponding to individual CTL clones), the mHag status of each HapMap LCL was defined as positive, negative, or undetermined.

To identify mHag loci, we performed association tests for all the Phase II HapMap SNPs, by calculating χ^2 test statistics based on 2 × 2 contingency tables with regard to the mHag status as measured by CRA and the HapMap genotypes (presence or absence of a particular allele) at each locus. χ^2 were calculated for the 2 possible mHag alleles at each locus and the larger value was adopted for each SNP. While different test statistics may be used showing different performance, the χ^2 statistic is most convenient for the purpose of power estimation as described below. The maximum value of the χ^2 statistics was evaluated against the thresholds empirically calculated from 100 000 random permutations within a given LCL set. The program was written in C++ and will run on a unix clone. It will be freely distributed on request. Computation of the statistics was performed within several seconds on a Macintosh equipped with 2 × quadcore 3.2 GHz Zeon processors (Apple, Cupertino, CA), although 100 000 permutations took several hours on average.

Evaluation of the power of association tests using HapMap samples

The genotyping data of the Phase II HapMap[14] were obtained from the International HapMap Project website (http://www.hapmap.org/genotypes/latest_ncbi_build35), among which we used the nonredundant data sets (excluding SNPs on the Y chromosome) from 60 CEU (Utah residents with ancestry from northern and western Europe) parents, 60 YRI (Yoruba in Ibadan, Nigeria) parents, and the combined set of 45 JPT (Japanese in Tokyo, Japan) and 45 CHB (Han Chinese in Beijing, China) unrelated people. They contained 3 901 416 (2 624 947 polymorphic), 3 843 537 (295 293 polymorphic), and 3 933 720 (2 516 310 polymorphic) SNPs for CEU, YRI, and JPT + CHB, respectively.

To evaluate the power, we first assumed that the Phase II HapMap SNP set contains the target SNP of the relevant mHag or its complete proxies, and that the immunologic assays can completely discriminate i $mHag^+$ and j $mHag^-$ HapMap LCLs. Under this ideal condition, the test statistic, or χ^2, for these SNPs takes a definite value, $f(i,j) = i+j$, which was compared with the maximum χ^2 value, or its distribution, under the null hypothesis, that is, no SNPs within the Phase II HapMap set should be associated with the mHag locus. Unfortunately, the latter distribution cannot be calculated in an explicit analytical form but needs to be empirically determined based on HapMap data, because Phase II HapMap SNPs are mutually interdependent due to extensive linkage disequilibrium within human populations. For this purpose, we simulated 10 000 case-control panels by randomly choosing i $mHag^+$ and j $mHag^-$ HapMap LCLs for various combinations of (i,j) and calculated the maximum χ^2 values (χ^2_{max}) for each panel to identify those (i,j) combinations, in which $f(i,j)$ exceeds the upper 1 percentile point of the simulated 10 000 maximum values, $g(i,j)^{P=.01}$.

When proxies are not complete (ie, $r^2 < 1$), the expected values will be decayed by the factor of r^2, and further reduced due to the probabilities of false positive (f_P) and negative (f_N) assays, and expressed as $\hat{f}(i,j) = (i+j) \times \hat{r}^2$ through an apparent r^2 ($\hat{r}^2$) as provided in formula 1.[1] Under given probabilities of assay errors and maximum LD strength between markers and the mHag allele, we can expect to identify target mHag loci for those (i,j) sets that satisfy $\hat{f}(i,j) > g(i,j)^{P=.01}$.

Empirical estimation of distributions of r^2

The maximum r^2 value (r^2_{max}) between a given mHag allele and one or more Phase II HapMap SNPs was estimated based on the observed HapMap data set. Each Phase II HapMap SNP was assumed to represent a target mHag allele, and the (r^2_{max}) was calculated, taking into account all the Phase II HapMap SNPs less than 500 kb apart from the target SNP.

Confirmatory genotyping

Genotyping was carried out either by TaqMan MGB technology (Applied Biosystems, Foster City, CA) with primers and probes for HA-1 mHag according to the manufacturer's protocol using an ABI 7900HT with the aid of SDS version 2.2 software (Applied Biosystems) or by direct sequencing of amplified cDNA for the *SLC1A5* gene. cDNA was reverse transcribed from total RNA extracted from LCLs, and polymerase chain reaction (PCR) was conducted with cDNA with the corresponding primers. Amplified DNA samples were sequenced using BigDye Terminator version 3.1 (Applied Biosystems). The presence or absence (deletion) of the *UGT2B17* gene was confirmed by genomic PCR with 2 primer sets for exons 1 and 6 as described previously[18] using DNA isolated from LCLs of interest.

Epitope mapping

A series of deletion mutant cDNAs were designed and cloned into pcDNA3.1/V5-His TOPO plasmid (Invitrogen, Carlsbad, CA). Thereafter, 293T cells that had been transduced with restricting HLA class I cDNA for individual CTL clones were transfected with each of the deletion mutants and cocultured with the CTL clone overnight to induce interferon (IFN)-γ release, which was then evaluated by enzyme-linked immunosorbent assay (ELISA) as previously described.[9]

For *SLC1A5*, expression plasmids encoding full-length cDNA and the exon 1 of recipient and donor origin were first constructed because only the SNP in the exon 1 was found to be concordant with susceptibility to CTL-3B6. Next, amino (N)- and (carboxyl) C-terminus–truncated mini-genes encoding polypeptides around the polymorphic amino acid defined by the SNP were amplified by PCR from *SLC1A5* exon 1 cDNA as template and cloned into the above plasmid. The constructs all encoded a Kozak

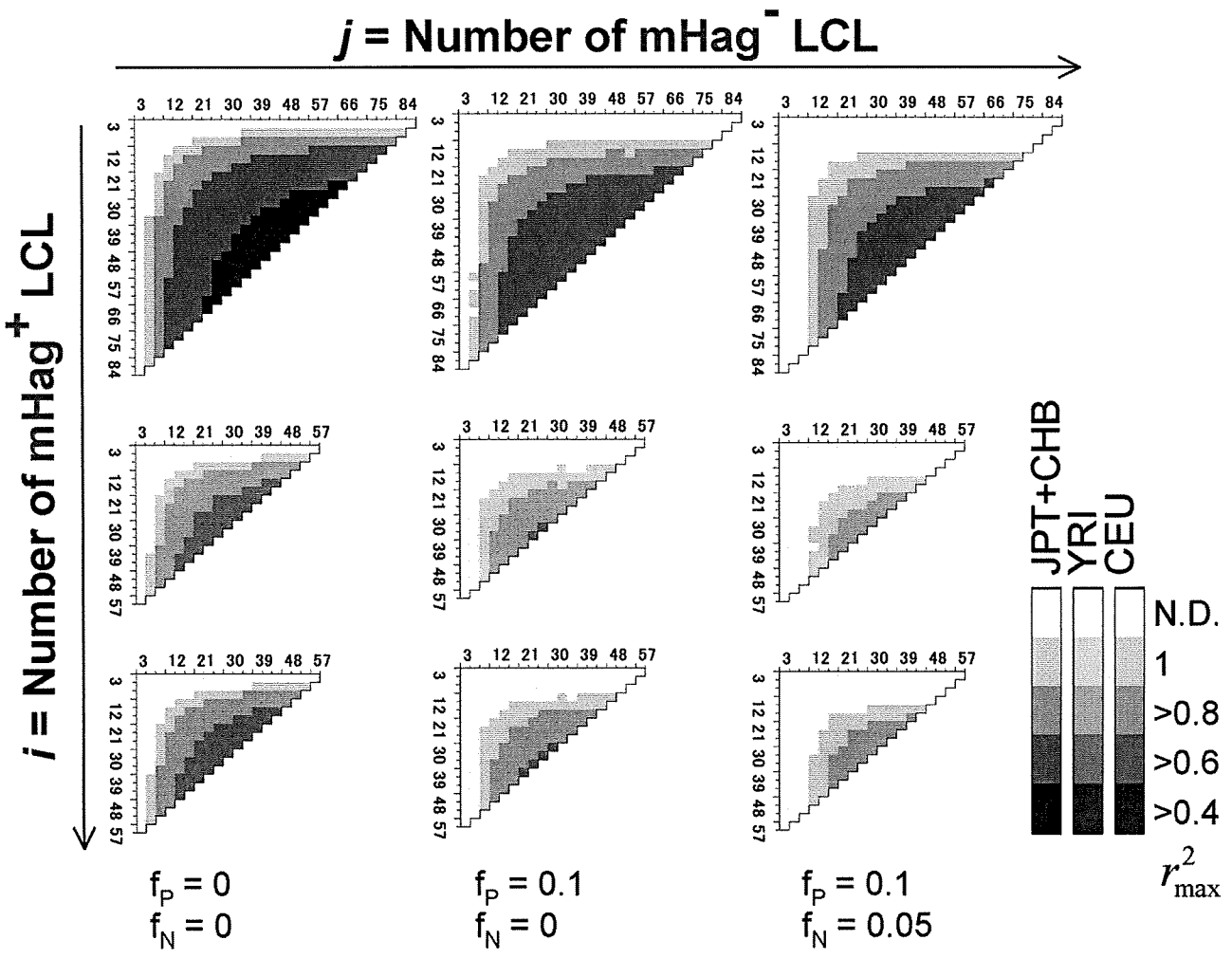

Figure 1. Numbers of positive and negative LCLs required for successful mHag mapping. The target locus was assumed to be uniquely identified, if the expected χ^2 value for the target SNP ($\hat{f}(i,j)$, see Document S1) exceeded the upper 1 percentile point of the maximum χ^2 values in 10 000 simulated case-control panels ($g(i,j)^{P=.01}$). Combinations of the numbers of mHag$^+$ (vertical coordinates) and mHag$^-$ (horizontal coordinates) samples satisfying the above condition are shown in color gradients corresponding to different max r^2 values between the target SNP and one or more nearby Phase II HapMap SNPs (r^2_{max}), ranging from 0.4 to 1.0. Calculations were made for 3 HapMap population panels, CHB + JPT (top), YRI (middle), and CEU (bottom) and for different false positive and negative rates, $f_P = f_N = 0$ (left), $f_P = 0.1, f_N \cong 0$ (middle), and $f_P = 0.1, f_N = 0.05$ (right), considering the very low false negative assays for CRAs.

sequence and initiator methionine (CCACC-ATG) and for C-terminus deletions a stop codon (TAG).

For *UGT2B17*, a series of C-terminus deletion mutants with approximately 200 bp spacing was first constructed as above. For further mapping, N-terminus deletion mutants were added to the region that was deduced to be potentially encoding the CTL-1B2 epitope. For prediction of a CTL epitope, the HLA Peptide Binding Predictions algorithm on the BioInformatics & Molecular Analysis Section (BIMAS) website (http://www.bimas.cit.nih.gov/molbio/hla_bind/)[19] was used because HLA-A*0206 has a similar binding motif to that of A*0201.

Epitope reconstitution assay

The candidate mHag epitopes and allelic counterpart peptides (in case of SLC1A5) were synthesized by standard Fmoc chemistry. ^{51}Cr-labeled mHag$^-$ donor LCL were incubated with graded concentrations of the peptides and then used as targets in standard CRAs.

Results and discussion

Statistical approach and estimation of potential overfitting

We reasoned that the mHag locus recognized by a given CTL clone could be defined by grouping LCLs from a HapMap panel into mHag$^+$ and mHag$^-$ subpanels according to their susceptibility to lysis by the CTL clone and then performing an association scan using the highly qualified HapMap data set containing more than 3 000 000 SNP markers. The relevant genetic trait here is expected to show near-complete penetrance, and the major concern with this approach arises from the risk of overfitting observed phenotypes to one or more incidental SNPs with this large number of HapMap SNPs under the relatively limited size of freedom due to small numbers of independent HapMap samples (90 for JPT + CHB and 60 for CEU and YRI, when not including their offspring).[13]

To address this problem, we first estimated the maximum sizes of the test statistics (here, χ^2 values) under the null hypothesis (ie, no associated SNPs within the HapMap set) by simulating 10 000 case-control HapMap panels under different experimental conditions, and compared them with the expected size of test statistic values from the marker SNPs associated with the target SNP, assuming different linkage disequilibrium (LD), or r^2 values in between. As shown in Figure 1, the possibility of overfitting became progressively reduced as the number of LCLs increased, which would allow for identification of the target locus in a broad range of r^2 values, except for those mHags having very low minor allele frequencies (MAF) below

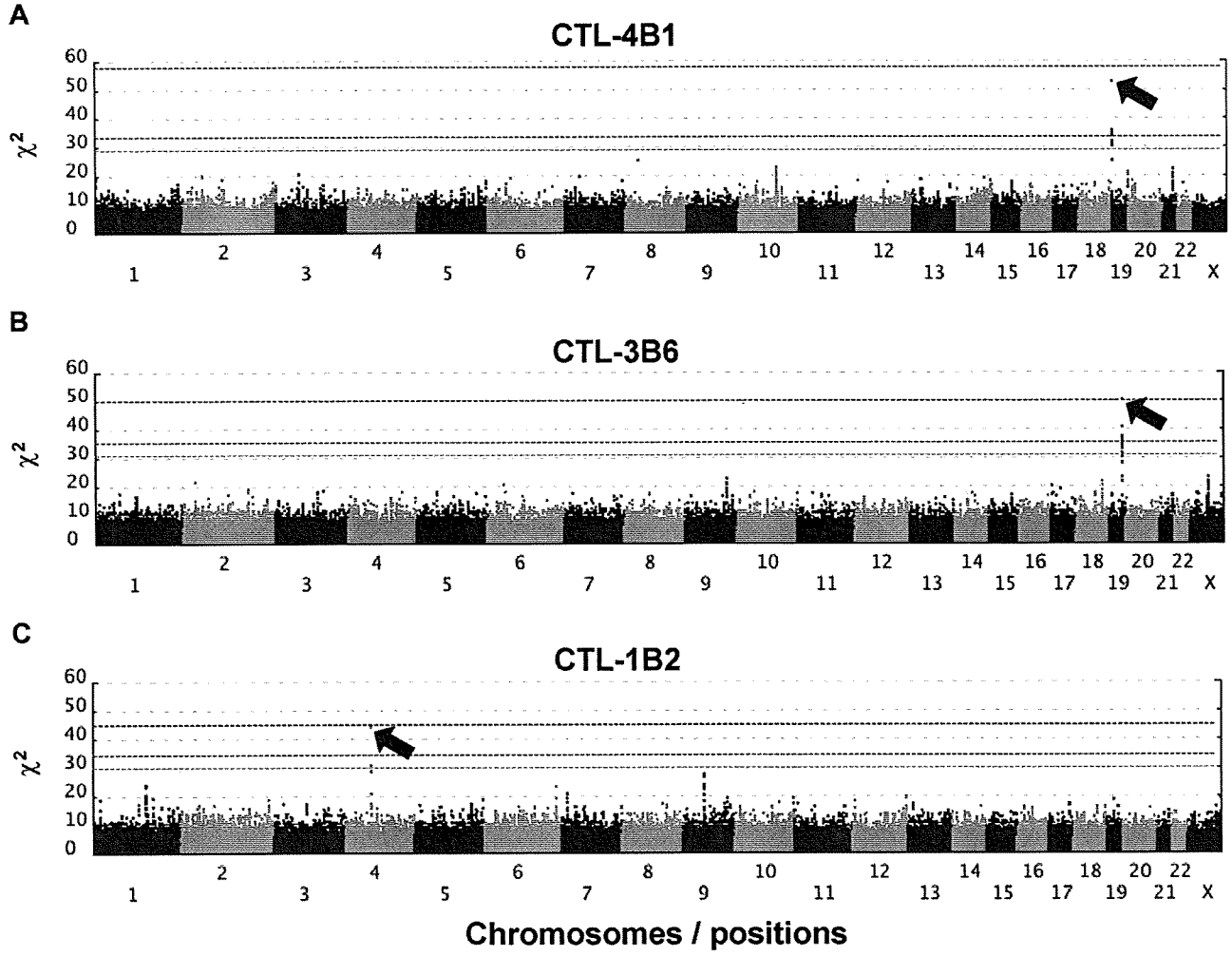

Figure 2. Genome-wide scanning to identify chromosome location of mHag. χ^2 values were plotted against positions on each chromosome for each of 3 mHags recognized by CTL-4B1 (A), CTL-3B6 (B), and CTL-1B2 (C). Chromosomes are displayed in alternating colors. Threshold χ^2 values corresponding to the genome-wide $P = 10^{-3}$ (dark blue) and 10^{-2} (light blue), as empirically determined from 100 000 random permutations, are indicated by broken lines, while the theoretically possible maximum values are shown with red broken lines. The highest χ^2 value in each experiment is indicated by a red arrow.

approximately 0.05. According to our estimation using the Phase II HapMap data (see "Methods"), the majority (> 90%) of common target SNPs (MAF > ~ 0.05) could be captured by one or more HapMap SNPs with more than 0.8 of r^2 (Figure S1, available on the *Blood* website; see the Supplemental Materials link at the top of the online article), ensuring a high probability of detecting an association (Figure 1 left panels). The simulation of pseudo-Phase II sets generated from the ENCODE regions provided a similar estimation.[13] False positive and negative immunophenotyping results could also complicate the detection, reducing the expected test statistics through the "apparent" r^2 values ($\hat{r}^2$), as defined by

$$\hat{r}^2 = r^2 \times \frac{(1 - f_P - f_N)^2}{(1 - f_P + f_N q)(1 - f_N + f_P/q)} \quad (1)$$

where f_P, f_N, and q represent false typing probabilities with positive and negative LCL panels, and the ratio of the positive to the negative LCL number, respectively. However, the high precision of cytotoxicity assays (f_P ~ < 0.1, f_N ~ = 0) limits this drawback from the second term to within acceptable levels and allows for sensitive mHag locus mapping with practical sample sizes (Figure 1 middle and right panels), suggesting the robustness of our novel approach.

Evaluation of the detection power for known mHags

Based on these considerations, we then assessed whether this approach could be used to correctly pinpoint known mHag loci (Table S1). Because the relevant mHag alleles are common SNPs and directly genotyped in the Phase II HapMap set, or if not, located within a well-defined LD block recognized in this set (Figure S2), their loci would be expected to be uniquely determined with an acceptable number of samples, as predicted from Figure 1. To test this experimentally, we first mapped the locus for HA-1^H mHag[7] by evaluating recognition of the HLA-A*0206–transduced HapMap cell panel with HLA-A*0206–restricted CTL-4B1.[20] After screening 58 well-growing LCLs from the JPT + CHB panel with CRAs using CTL-4B1 (Figure S3A; Tables S2,S3), we obtained 37 mHag$^+$ and 21 mHag$^-$ LCLs, which were tested for association at 3 933 720 SNP loci. The SNP (rs1801284) encoding the mHag is located within a HapMap LD block on chromosome 19q13.3, but is not directly genotyped within this data set. The genome-wide scan clearly indicated a unique association with the HA-1^H locus within the *HMHA1* gene, showing a peak χ^2 statistic of 52.8 (not reached in 100 000 permutations) at rs10421359 (Figures 2A,3A; Tables S2,S3).

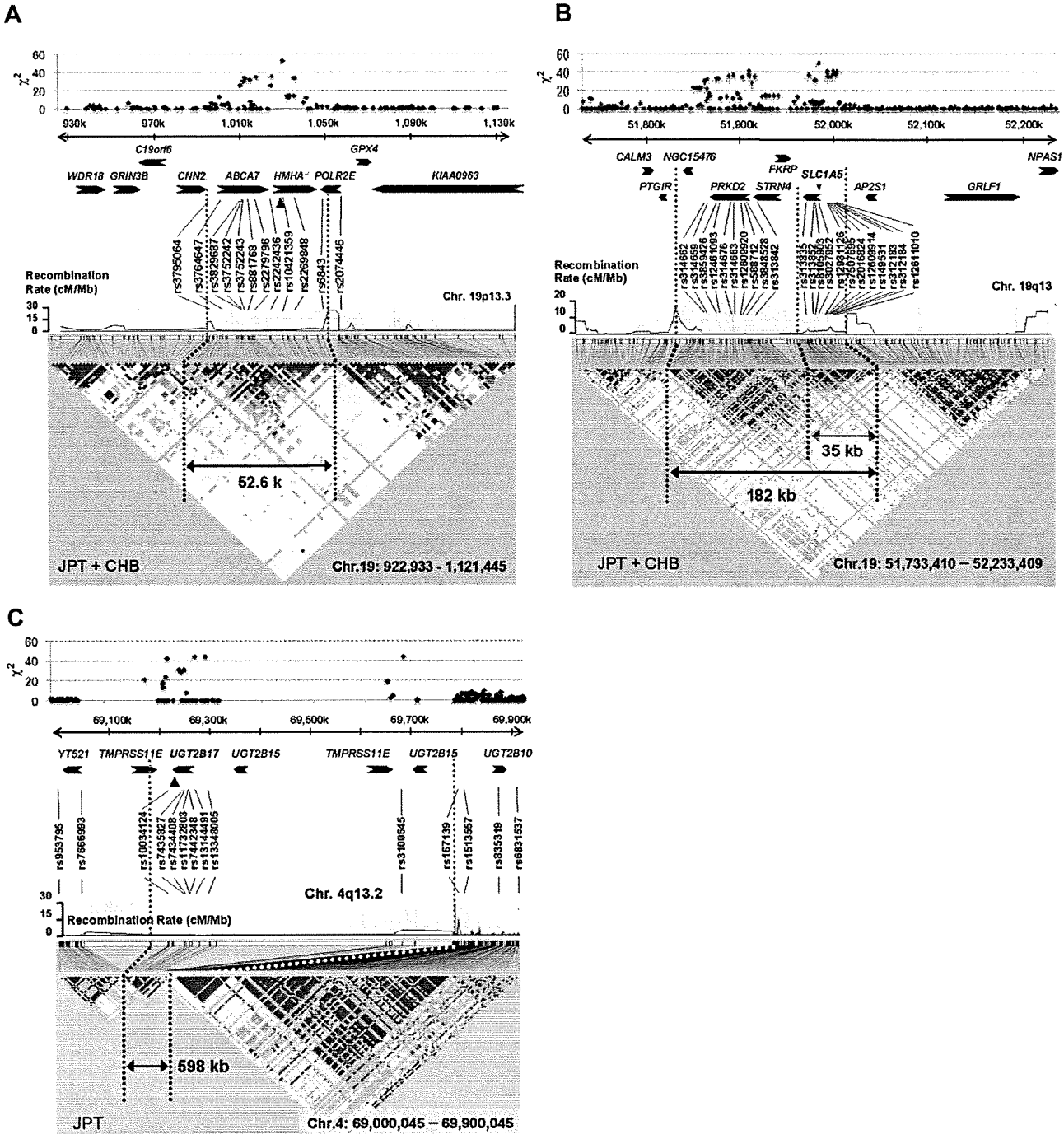

Figure 3. Regions of mHag loci identified by HapMap scanning. LD structures around the SNPs showing peak statistical values (in JPT + CHB) are presented for each mHag locus identified with (A) CTL-4B1, (B) CTL-3B6, and (C) CTL-1B2. Regional χ^2 plots are also provided on the top of each panel. LD plots in pairwise D's with recombination rates along the segment were drawn with HaploView software version 4.0 (http://www.broad.mit.edu/mpg/haploview/). The size and location of each LD block containing a mHag locus are indicated within the panels. Significant SNPs (blue letters), as well as other representative SNPs, are shown in relation to known genes. The positions of the SNPs showing the highest statistic values (red letters) are indicated by red arrowheads.

Identification of novel mHags

We next applied this method to mapping novel mHags recognized by CTL clone 3B6, which is HLA-B*4002–restricted; and CTL clone 1B2, which is HLA-A*0206–restricted. Both clones had been isolated from peripheral blood samples of post-HSCT different patients. In preliminary CRAs with the JPT + CHB panel, allele frequencies of target mHags for CTL-3B6 and CTL-1B2 in this panel were estimated as approximately 25% and approximately 45%, respectively (data not shown). After screening 72 JPT + CHB LCLs with CTL-3B6, 36 mHag$^+$ and 14 mHag$^-$ LCLs were obtained, leaving 22 LCLs undetermined based on empirically determined thresholds (> 51% for mHag + LCLs and < 11% for mHag-LCLs; Figure S3B, Tables S2,S4). As shown in Figure 2B, the χ^2 statistics calculated from the immunophenotyping data produced discrete peaks in the LCL sets. The peak in chromosome 19q13.3 for the CTL-3B6 set showed the theoretically maximum χ^2 value of 50 (not reached in 100 000 permutations) at rs3027952, which was mapped within a small LD block of

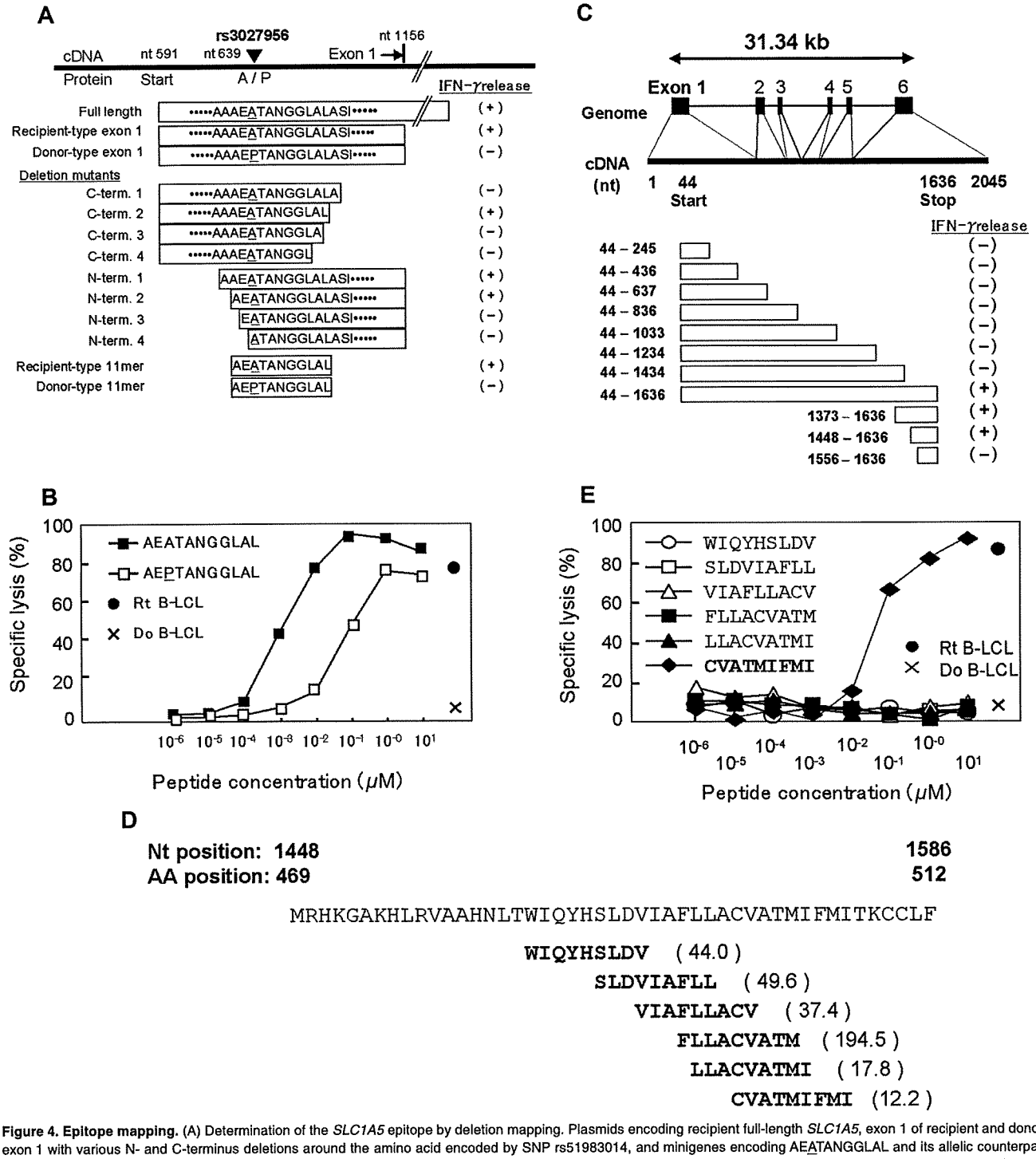

Figure 4. Epitope mapping. (A) Determination of the *SLC1A5* epitope by deletion mapping. Plasmids encoding recipient full-length *SLC1A5*, exon 1 of recipient and donor, exon 1 with various N- and C-terminus deletions around the amino acid encoded by SNP rs51983014, and minigenes encoding AEATANGGLAL and its allelic counterpart AEPTANGGLAL were constructed and transfected into HLA-B*4002–transduced 293T cells. Interferon (IFN)-γ was assessed by ELISA (right column) after coculture of CTL-3B1 with 293T transfectants. (B) Epitope reconstitution assay with synthetic undecameric peptides, AEATANGGLAL and AEPTANGGLAL. (C) Structure of the *UGT2B17* gene and screening of *UGT2B17* cDNA and deletion mutants. HLA-A*0206–transduced 293T cells were transfected with each plasmid and cocultured with CTL-2B1. IFN-γ production from CTL-1B2 (right column) indicated that the epitope was likely encoded by nucleotides 1448-1586, including 30 nucleotides from position 1566 that could potentially encode part of the epitope. (D) Epitope prediction using the HLA Peptide Binding Predictions algorithm.[19] Because HLA-A*0201 and -A*0206 have similar peptide binding motifs,[30] the algorithm for HLA-A*0201 was used to predict candidate epitopes recognized by CTL-1B2. Values in parentheses indicate the predicted half-time of dissociation. (E) Epitope reconstitution assays with graded concentrations of synthetic nonameric peptides shown in panel D.

approximately 182 kb, or more narrowly within its 35 kb sub-block containing a single gene, *SLC1A5*, as a candidate mHag gene (Figure 3B). In fact, when expressed in 293T cells with HLA-B*4002 transgene, recipient-derived, but not donor-derived, *SLC1A5* cDNA was able to stimulate IFN-γ secretion from CTL-3B6 (Figure 4A), indicating that *SLC1A5* actually encodes the target mHag recognized by CTL-3B6. Conventional epitope mapping using a series of deletion mutants of *SLC1A5* cDNA finally identified an undecameric peptide, AEATANGGLAL, as the minimal epitope (Figure 4A). The donor-type AEPTANGGLAL induced IFN-γ with a 2-log lower efficiency, suggesting that AEPTANGGLAL may not be transported efficiently into the ER

because endogenous expression of a minigene encoding AEPTANGGLAL was not recognized by CTL-3B1 (Figure 4B). Unfortunately, although the peak statistic value showed the theoretically maximum value for this data set, it did not conform to the relevant SNP for this mHag (rs3027956) due to high genotyping errors of the HapMap data at this particular SNP. However, the result of our resequencing showed complete concordance with the presence of the rs3027956 SNP and recognition in the cytotoxicity assay (Table S4).

Similarly, 13 $mHag^+$ and 32 $mHag^-$ LCLs were identified from the screening of 45 JPT LCLs from the same panel using CTL-1B2 (Figure S3C; Tables S2,S5). The χ^2 statistics calculated from the immunophenotyping data produced bimodal discrete peaks with this LCL set. The target locus for the mHag recognized by CTL-1B2 was identified at a peak (max $\chi^2 = 44$, not reached in 100 000 permutations) within a 598-kb block on chromosome 4q13.1, coinciding with the locus for a previously reported mHag, *UGT2B17*[18] (Figures 2C, 3C). In fact, our epitope mapping using *UGT2B17* cDNA deletion mutants (Figure 4C), prediction of candidate epitopes by HLA-binding algorithms[19] (Figure 4D) and epitope reconstitution assays (Figure 4E), successfully identified a novel nonameric peptide, CVATMIFMI. Of particular note, this mHag was not defined by a SNP but by a CNV (ie, a null allele[18]) that is in complete LD with the SNPs showing the maximum χ^2 value (Table S5). Transplanted T cells from donors lacking both *UGT2B17* alleles are sensitized in recipients possessing at least 1 copy of this gene.[18] Although LD between SNPs and CNVs has been reported to be less prominent,[21] this is an example where a CNV trait could be captured by a SNP-based genome-wide association study.

The recent generation of the HapMap has had a profound impact on human genetics.[13,15] In the field of medical genetics, the HapMap is a central resource for the development of theories and methods that have made well-powered, genome-wide association studies of common human diseases a reality.[22-28] The HapMap samples provide not only an invaluable reference for genetic variations within human populations, but highly qualified genotypes that enable gene-wide scanning. Here, we have demonstrated how effectively HapMap resources can be used for genetic mapping of clinically relevant human traits. No imputations and tagging strategies are required[25,28] and the potential loss of statistical power due to very limited sample sizes is circumvented by accurate immunologic detection of the traits.

Using publicly available HapMap resources, high-throughput identification of mHag genes is possible without highly specialized equipment or expensive microarrays. Except for clinically irrelevant mHags with very low allele frequencies (eg, MAF $< 5\%$), the target of a given CTL can be sensitively mapped within a mean LD block size, typically containing just a few candidate genes. The methodology described here will facilitate construction of a large panel of human mHags including those presented by MHC class II molecules, and promote our understanding of human allo-immunity and development of targeted allo-immune therapies for hematologic malignancies.[1,2] The HapMap scan approach may be useful for exploring other genetic traits or molecular targets (eg, differential responses to some stress or drugs), if they can be discriminated accurately through appropriate biologic assays. In this context, the recent report that we may reprogram the fate of terminally differentiated human cells[29] is encouraging, indicating possible exploration of genotypes that are relevant to cell types other than immortalized B cells.

Acknowledgments

We thank Drs P. Martin and W. Ho for critically reading the manuscript; and Ms Keiko Nishida, Dr Ayako Demachi-Okamura, Dr Yukiko Watanabe, Ms Hiromi Tamaki, and the staff members of the transplant centers for their generous cooperation and technical expertise.

This study was supported in part by a grant for Scientific Research on Priority Areas (B01; no.17016089) from the Ministry of Education, Culture, Science, Sports, and Technology, Japan; grants for Research on the Human Genome, Tissue Engineering Food Biotechnology and the Second and Third Team Comprehensive 10-year Strategy for Cancer Control (no. 26) from the Ministry of Health, Labor, and Welfare, Japan; and a grant-in-aid from Core Research for Evolutional Science and Technology (CREST) of Japan.

Authorship

Contribution: M.K. performed most of immunologic experiments and analyzed data and wrote the manuscript; Y.N. performed the majority of genetic analyses and analyzed the data; H.T., T.K., M.Y., S.M. and K.Tsujimura performed research; K.Taura contributed to the computational simulation; Y.I., Taro T., K.M., Y.K. and Y.M. collected clinical data and specimens; T.I., H.T., S.R.R., Toshitada T. and K.K. contributed to data analysis and interpretation, and writing of the article; and Y.A. and S.O. supervised the entire project, designed and coordinated most of the experiments in this study, and contributed to manuscript preparation.

Conflict-of-interest disclosure: The authors declare no competing financial interests.

Correspondence: Seishi Ogawa, MD, PhD, Department of Hematology and Oncology, Department of Regeneration Medicine for Hematopoiesis, The 21st Century COE Program, Graduate School of Medicine, University of Tokyo, 7-3-1, Hongo, Bunkyo-ku, Tokyo 113-8655, Japan; e-mail: sogawa-tky@umin.ac.jp; or Yoshiki Akatsuka, MD, PhD, Division of Immunology, Aichi Cancer Center Research Institute, 1-1 Kanokoden, Chikusa-ku, Nagoya 464-8681, Japan; e-mail: yakatsuk@aichi-cc.jp.

References

1. Bleakley M, Riddell SR. Molecules and mechanisms of the graft-versus-leukaemia effect. Nat Rev Cancer. 2004;4:371-380.
2. Spierings E, Goulmy E. Expanding the immunotherapeutic potential of minor histocompatibility antigens. J Clin Invest. 2005;115:3397-3400.
3. de Rijke B, van Horssen-Zoetbrood A, Beekman JM, et al. A frameshift polymorphism in P2X5 elicits an allogeneic cytotoxic T lymphocyte response associated with remission of chronic myeloid leukemia. J Clin Invest. 2005;115:3506-3516.
4. Marijt WA, Heemskerk MH, Kloosterboer FM, et al. Hematopoiesis-restricted minor histocompatibility antigens HA-1- or HA-2-specific T cells can induce complete remissions of relapsed leukemia. Proc Natl Acad Sci U S A. 2003;100:2742-2747.
5. Spierings E, Hendriks M, Absi L, et al. Phenotype frequencies of autosomal minor histocompatibility antigens display significant differences among populations. PLoS Genet. 2007;3:e103.
6. Brickner AG, Warren EH, Caldwell JA, et al. The immunogenicity of a new human minor histocompatibility antigen results from differential antigen processing. J Exp Med. 2001;193:195-206.
7. den Haan JM, Meadows LM, Wang W, et al. The minor histocompatibility antigen HA-1: a diallelic gene with a single amino acid polymorphism. Science. 1998;279:1054-1057.

8. Dolstra H, Fredrix H, Maas F, et al. A human minor histocompatibility antigen specific for B cell acute lymphoblastic leukemia. J Exp Med. 1999; 189:301-308.
9. Kawase T, Akatsuka Y, Torikai H, et al. Alternative splicing due to an intronic SNP in HMSD generates a novel minor histocompatibility antigen. Blood. 2007;110:1055-1063.
10. Akatsuka Y, Nishida T, Kondo E, et al. Identification of a polymorphic gene, BCL2A1, encoding two novel hematopoietic lineage-specific minor histocompatibility antigens. J Exp Med. 2003;197: 1489-1500.
11. Kawase T, Nanya Y, Torikai H, et al. Identification of human minor histocompatibility antigens based on genetic association with highly parallel genotyping of pooled DNA. Blood. 2008;111:3286-3294.
12. Risch N, Merikangas K. The future of genetic studies of complex human diseases. Science. 1996;273:1516-1517.
13. The International HapMap Consortium. The International HapMap Project. Nature. 2003;426:789-796.
14. The International HapMap Consortium. A second generation human haplotype map of over 3.1 million SNPs. Nature. 2007;449:851-861.
15. The International HapMap Consortium. A haplotype map of the human genome. Nature. 2005; 437:1299-1320.
16. Akatsuka Y, Goldberg TA, Kondo E, et al. Efficient cloning and expression of HLA class I cDNA in human B-lymphoblastoid cell lines. Tissue Antigens. 2002;59:502-511.
17. Riddell SR, Greenberg PD. The use of anti-CD3 and anti-CD28 monoclonal antibodies to clone and expand human antigen-specific T cells. J Immunol Methods. 1990;128:189-201.
18. Murata M, Warren EH, Riddell SR. A human minor histocompatibility antigen resulting from differential expression due to a gene deletion. J Exp Med. 2003;197:1279-1289.
19. Parker KC, Bednarek MA, Coligan JE. Scheme for ranking potential HLA-A2 binding peptides based on independent binding of individual peptide side-chains. J Immunol. 1994;152:163-175.
20. Torikai H, Akatsuka Y, Miyauchi H, et al. The HLA-A*0201-restricted minor histocompatibility antigen HA-1H peptide can also be presented by another HLA-A2 subtype, A*0206. Bone Marrow Transplant. 2007;40:165-174.
21. Redon R, Ishikawa S, Fitch KR, et al. Global variation in copy number in the human genome. Nature. 2006;444:444-454.
22. Barrett JC, Cardon LR. Evaluating coverage of genome-wide association studies. Nat Genet. 2006;38:659-662.
23. Nannya Y, Taura K, Kurokawa M, Chiba S, Ogawa S. Evaluation of genome-wide power of genetic association studies based on empirical data from the HapMap project. Hum Mol Genet. 2007;16:2494-2505.
24. Pe'er I, de Bakker PI, Maller J, Yelensky R, Altshuler D, Daly MJ. Evaluating and improving power in whole-genome association studies using fixed marker sets. Nat Genet. 2006;38:663-667.
25. Marchini J, Howie B, Myers S, McVean G, Donnelly P. A new multipoint method for genome-wide association studies by imputation of genotypes. Nat Genet. 2007;39:906-913.
26. Altshuler D, Daly M. Guilt beyond a reasonable doubt. Nat Genet. 2007;39:813-815.
27. Bowcock AM. Genomics: guilt by association. Nature. 2007;447:645-646.
28. de Bakker PI, Burtt NP, Graham RR, et al. Transferability of tag SNPs in genetic association studies in multiple populations. Nat Genet. 2006;38: 1298-1303.
29. Takahashi K, Tanabe K, Ohnuki M, et al. Induction of pluripotent stem cells from adult human fibroblasts by defined factors. Cell. 2007;131: 861-872.
30. Sudo T, Kamikawaji N, Kimura A, et al. Differences in MHC class I self peptide repertoires among HLA-A2 subtypes. J Immunol. 1995;155: 4749-4756.

blood

2009 113: 2096-2103
Prepublished online Jan 6, 2009;
doi:10.1182/blood-2008-03-145862

Hematopoietic stem cell transplantation for core binding factor acute myeloid leukemia: t(8;21) and inv(16) represent different clinical outcomes

Yachiyo Kuwatsuka, Koichi Miyamura, Ritsuro Suzuki, Masaharu Kasai, Atsuo Maruta, Hiroyasu Ogawa, Ryuji Tanosaki, Satoshi Takahashi, Kyuhei Koda, Kazuhiro Yago, Yoshiko Atsuta, Takashi Yoshida, Hisashi Sakamaki and Yoshihisa Kodera

Blood (print ISSN 0006-4971, online ISSN 1528-0020), is published semimonthly by the American Society of Hematology, 1900 M St, NW, Suite 200, Washington DC 20036.

Hematopoietic stem cell transplantation for core binding factor acute myeloid leukemia: t(8;21) and inv(16) represent different clinical outcomes

Yachiyo Kuwatsuka,[1] Koichi Miyamura,[1] Ritsuro Suzuki,[2] Masaharu Kasai,[3] Atsuo Maruta,[4] Hiroyasu Ogawa,[5] Ryuji Tanosaki,[6] Satoshi Takahashi,[7] Kyuhei Koda,[8] Kazuhiro Yago,[9] Yoshiko Atsuta,[2] Takashi Yoshida,[10] Hisashi Sakamaki,[11] and Yoshihisa Kodera[1]

[1]Department of Hematology, Japanese Red Cross Nagoya First Hospital, Nagoya; [2]Department of HSCT Data Management, Nagoya University School of Medicine, Nagoya; [3]Department of Hematology, Sapporo Hokuyu Hospital, Sapporo; [4]Department of Hematology, Kanagawa Cancer Center, Yokohama; [5]Department of Molecular Medicine, Osaka University Graduate School of Medicine, Osaka; [6]Stem Cell Transplantation Unit, National Cancer Center Hospital, Tokyo; [7]Department of Hematology, Institute of Medical Science, The University of Tokyo, Tokyo; [8]Department of Hematology, Asahikawa Red Cross Hospital, Asahikawa; [9]Department of Hematology, Shizuoka General Hospital, Shizuoka; [10]Hematology Department, Toyama Prefectural Hospital, Toyama; and [11]Department of Hematology, Tokyo Metropolitan Komagome Hospital, Tokyo, Japan

We analyzed 338 adult patients with acute myeloid leukemia (AML) with t(8;21) and inv(16) undergoing stem cell transplantation (SCT) who were registered in the Japan Society for Hematopoietic Cell Transplantation database. At 3 years, overall survival (OS) of patients with t(8;21) and inv(16) was 50% and 72%, respectively ($P = .002$). Although no difference was observed when restricted to allogeneic SCT in first complete remission (CR; 84% and 74%), OS of patients with t(8;21) and inv(16) undergoing allogeneic SCT in second or third CR (45% and 86% at 3 years; $P = .008$) was different. OS was not different between patients in first CR who received allogeneic SCT and those who received autologous SCT for both t(8;21) AML (84% vs 77%; $P = .49$) and inv(16) AML (74% vs 59%; $P = .86$). Patients with inv(16) not in CR did better after allogeneic SCT than those with t(8;21) (70% and 18%; $P = .03$). Patients with t(8;21) and inv(16) should be managed differently as to the application of SCT. SCT in first CR is not necessarily recommended for inv(16). For t(8;21) patients in first CR, a prospective trial is needed to clarify the significance of autologous SCT and allogeneic SCT over chemotherapy. (Blood. 2009;113:2096-2103)

Introduction

Core binding factor (CBF) acute myeloid leukemia (AML) including t(8;21)(q22;q22) and inv(16)(p13q22)/t(16;16)(p13;q22) [t(8;21) and inv(16)] is considered to be a favorable cytogenetic subgroup in clinical studies.[1-4] Patients with t(8;21) and inv(16) have shown a markedly improved outcome with repetitive use of high-dose cytarabine.[5-13] However, the major treatment failure is disease recurrence.[14-16] These patients frequently become stem cell transplantation (SCT) candidates.

Both t(8;21) and inv(16) AMLs are associated with disruption of genes encoding subunits of the CBF, a heterodimeric transcriptional factor involved in the regulation of hematopoiesis.[17,18] Although these 2 different cytogenetics also share common clinical characteristics, they are associated with different clinical features such as morphologic presentation and immunophenotypic marker expression.[19]

Several reports demonstrated inferior outcome of t(8;21) compared with inv(16), but the number of patients who underwent transplantation was limited.[14,15,20] A recent study from the Dana-Farber Cancer Institute reported that both patients with t(8;21) and inv(16) de novo AML who underwent allogeneic transplantation performed favorably compared with other karyotypes.[21] To identify the survival data and prognostic factors among the CBF leukemia population who received SCT, we conducted a retrospective analysis using a Japanese multi-institution database with a large number of patients.

Methods

Study population

A total of 2802 adult patients who underwent autologous or allogeneic SCT from 1996 and 2004 for AML were registered in the Japan Society for Hematopoietic Cell Transplantation (JSHCT) database. Patients who underwent SCT from unrelated donors were registered in the different registry in the study period, but not all of the patients undergoing unrelated SCT were registered in the JSHCT database. Demographic, diagnostic, clinical, cytogenetics, induction, and outcome information were collected for each patient, and were sent to a central registration center. Cytogenetic studies were performed in each center, but a central review of cytogenetic analysis was not performed.

Patients with de novo AML aged 16 to 70 years who received hematopoietic SCT as the first transplant were included in the study. No patients with prior history of autologous or allogeneic SCT were included in the study. Of the remaining 2164 patients, 178 patients with t(15;17) or PML/RARα were excluded from the analysis below (Table 1). Finally, of the 1986 patients included in the analysis, 255 were reported to have t(8;21) abnormality, and 83 to have inv(16). A total of 194 patients had no available cytogenetic data. The remaining 1454 patients with normal karyotype and other cytogenetic abnormalities were further coded and analyzed according to published Southwest Oncology Group (SWOG) criteria.[3] The intermediate risk category included patients characterized by +8, −Y, +6, del(12p), or normal karyotype. The unfavorable risk category was defined by the presence of one or more of −5/del(5q), −7/del(7q), abn 3q, 11q, 20q, or

Submitted March 18, 2008; accepted December 17, 2008. Prepublished online as *Blood* First Edition paper, January 6, 2009; DOI 10.1182/blood-2008-03-145862 .

The online version of this article contains a data supplement.

The publication costs of this article were defrayed in part by page charge payment. Therefore, and solely to indicate this fact, this article is hereby marked "advertisement" in accordance with 18 USC section 1734.

Table 1. Cytogenetic risk groups of patients with AML who received autologous SCT and allogeneic SCT

Cytogenetic risk groups	No. patients		
	Auto-SCT	Allo-SCT	Total
t(8;21)	61	194	255
inv(16)	17	66	83
t(15;17)*	65	113	178
Intermediate	140	749	889
Unfavorable	35	325	360
Unknown			
Unknown cytogenetic risk	27	178	205
No available cytogenetic data	44	150	194
Total	389	1775	2164

Auto-SCT indicates autologous stem cell transplantation; Allo-SCT, allogeneic stem cell transplantation.

*Patients with t(15;17) were excluded from the analysis.

21q, del(9q), t(6;9), t(9;22), abn 17p, and complex karyotypes defined as 3 or more abnormalities. Patients with other cytogenetic aberrations were considered an unknown risk group, and were analyzed together with 194 patients with no cytogenetic data.

This study was approved by the Committee for Nationwide Survey Data Management of the JSHCT. Informed consent was obtained in accordance with the Declaration of Helsinki.

Transplantation

A total of 1662 patients underwent allogeneic SCT, and 324 underwent autologous SCT. Patients were treated with various conditioning regimens, but most of those who underwent autologous transplantation received non–total body irradiation (TBI) regimens (97%), including busulfan (BU), cytarabine (CA), and etoposide. The most frequently used conditioning regimens before allogeneic SCT were cyclophosphamide (Cy) plus TBI (n = 327 patients), and BU plus Cy (n = 267). Conditioning regimens before allogeneic SCT also included more intensified regimens such as CA plus Cy plus TBI (n = 262) and BU plus Cy plus TBI (n = 146), or reduced-intensity conditioning regimens with fludarabine (n = 241) or cladribine (n = 19).

Stem cell sources for allogeneic SCT were bone marrow in 871 patients, peripheral blood stem cell in 570 patients, bone marrow plus peripheral blood stem cell in 23 patients, and cord blood in 190 patients. A total of 1242 patients underwent allogeneic SCT from a related donor, and 404 patients underwent SCT from an unrelated donor.

Of the 1637 patients who had available data, 74% received transplants from human leukocyte antigen (HLA)–matched donors. Among patients who received unrelated bone marrow transplants, 156 patients were HLA genotypically matched and 51 were HLA mismatched. HLA data for 39 mismatched unrelated bone marrow transplantation patients were available. A total of 32 patients were one locus mismatched, and 7 patients were 2 loci mismatched. Among patients receiving unrelated cord blood transplants, 19 patients were serologically HLA matched and 170 patients were mismatched. HLA incompatibility was 5 of 6 HLA matched in 57 patients, 4 of 6 HLA matched in 99 patients, 3 of 6 HLA matched in 7 patients, and 1 of 6 HLA matched in 1 patient.

Graft-versus-host disease (GVHD) prophylaxis mostly consisted of methotrexate and a calcineurin inhibitor, either cyclosporin A or tacrolimus. Several other prophylaxes include mycophenolate mofetil, antithymocyte globulin, and $CD34^+$ selection. The incidence of acute GVHD was evaluated in 1488 patients who survived more than 28 days, and chronic GVHD was evaluated in 1302 patients who survived more than 100 days after allogeneic SCT. GVHD was evaluated in each center.

Statistical analysis

Correlation between the 2 groups was examined with the chi-square test, Fisher exact test, and the Mann-Whitney *U* test. Disease-free survival (DFS) was calculated from the date of transplantation until the date of relapse or the date of death in CR. Patient survival data were analyzed with the method of Kaplan and Meier and compared by the log-rank test.

Univariate and multivariate analyses for OS were performed with the aid of the Cox proportional hazard regression model, and variables were selected with the stepwise method. The following variables were evaluated: age, sex, and disease status at transplantation; CR versus not in CR; the number of induction courses to achieve CR; one course versus more than one course and failure; type of transplantation (allogeneic SCT vs autologous SCT); conditioning regimen (reduced intensity vs myeloablative); TBI regimen or not; and the existence of additional karyotype abnormalities or not. For those who received allogeneic SCT, in addition to these variables, the following were also evaluated: type of GVHD prophylaxis; short-course methotrexate plus cyclosporin A or short methotrexate plus FK506; acute GVHD, grade II to IV or grade III to IV; chronic GVHD; HLA mismatch; donor; and donor source. The doses of methotrexate were not surveyed. Each factor was considered to be prognostic if the *P* value was less than .05. Data were analyzed with the Stata 9.2 statistical software (College Station, TX).

Results

Initial characteristics of patients

The median age of all patients with AML in total was 41 years old (range, 16-70 years old). Median follow-up period of living patients was 37.3 months (range, 0.4-108 months). Patients were categorized into 5 cytogenetic subgroups: with t(8;21), with inv(16), intermediate risk cytogenetics, unfavorable cytogenetics, and an unknown risk group. Table 1 shows the number of patients in each cytogenetic subgroup and patients with t(15;17), who were excluded from the analysis.

Characteristics of the patients with CBF who underwent allogeneic SCT or autologous SCT are shown in Table 2. No significant difference was observed between characteristic of 2 groups of patients with CBF who received autologous SCT, except for the initial white blood cell count.

Of the 259 patients with CBF who received allogeneic SCT, significantly more patients with t(8;21) had failed to achieve CR with a single course of induction chemotherapy at diagnosis ($P = .002$), and were not in CR at the time of transplantation ($P < .001$). Among patients in CR at transplantation, the ratio of those in first, second, or third CR was not different between t(8;21) and inv(16) subgroups. Significantly more patients with inv(16) received transplants from an unrelated donor ($P = .004$). Table 3 and Table S1 (available on the *Blood* website; see the Supplemental Materials link at the top of the online article) summarize the transplantation data of those undergoing allogeneic SCT. More patients with inv(16) received unrelated transplants compared with t(8;21) patients ($P = .004$).

Overall survival

The OS of 1986 patients with AML at 3 years was 48%, and those with t(8;21), inv(16), intermediate, unfavorable, and unknown cytogenetic risks showed OS of 50%, 72%, 52%, 35%, and 45%, respectively ($P < .001$). Figure 1 shows survival curves of patients with AML patients who underwent allogeneic SCT in first CR (Figure 1A), in second or third CR (Figure 1B), or not in CR (Figure 1C), categorized by the cytogenetic abnormalities. Survival data are listed in Table 4. The OS of patients with t(8;21), inv(16), and intermediate, unfavorable, and unknown risk undergoing allogeneic SCT in first CR was 84%, 74%, 69%, 53%, and 52%, respectively ($P < .001$), and that of patients undergoing allogeneic-SCT